



AFTAC Project No. VT/1705

RESOLUTION AND STABILITY OF WAVENUMBER  
SPECTRAL ESTIMATES

SPECIAL REPORT NO. 2  
EXTENDED ARRAY EVALUATION PROGRAM

Prepared by Aaron H. Booker and Chung-yen Ong

T. W. Harley, Program Manager  
Area Code 703, 836-3882 Ext. 300

TEXAS INSTRUMENTS INCORPORATED  
Services Group  
P.O. Box 5621  
Dallas, Texas 75222

Contract No. F33657-71-C-0843  
Amount of Contract: \$511,580  
Beginning 1 April 1971  
Ending 31 March 1972

Prepared for  
AIR FORCE TECHNICAL APPLICATIONS CENTER  
Washington, D.C. 20333

Sponsored by  
ADVANCED RESEARCH PROJECTS AGENCY  
Nuclear Monitoring Research Office  
ARPA Order No. 1714  
ARPA Program Code No. 1F10

30 April 1972

Acknowledgement: This research was supported by the Advanced Research Projects Agency, Nuclear Monitoring Research Office, under Project VELA-UNIFORM, and accomplished under the technical direction of the Air Force Technical Applications Center under Contract No. F33657-71-C-0843.

AD 745195

49

UNCLASSIFIED

Security Classification

DOCUMENT CONTROL DATA - R & D

(Security classification of title, body of abstract and indexing annotation must be entered when the overall report is classified)

1. ORIGINATING ACTIVITY (Corporate author) Texas Instruments Incorporated Services Group P.O. Box 5621, Dallas, Texas 75222		2a. REPORT SECURITY CLASSIFICATION	
		2b. GROUP	
3. REPORT TITLE Resolution and Stability of Spectral Estimates, Special Report No. 2, Extended Array Evaluation Program			
4. DESCRIPTIVE NOTES (Type of report and inclusive dates) Special			
5. AUTHOR(S) (First name, middle initial, last name) Aaron H. Booker and Chung-yen Ong			
6. REPORT DATE 15 March 1972	7a. TOTAL NO. OF PAGES 45	7b. NO. OF REFS 4	
8a. CONTRACT OR GRANT NO. Contract No. F33657-71-C-0843	9a. ORIGINATOR'S REPORT NUMBER(S)		
b. PROJECT NO. AFTAC Project No. VT/1705	9b. OTHER REPORT NO(S) (Any other numbers that may be assigned this report)		
c.			
d.			
10. DISTRIBUTION STATEMENT APPROVED FOR PUBLIC RELEASE; DISTRIBUTION UNLIMITED			
11. SUPPLEMENTARY NOTES		12. SPONSORING MILITARY ACTIVITY Advanced Research Projects Agency Department of Defense The Pentagon, Washington, D. C. 20301	
13. ABSTRACT  -The relative resolution and stability of conventional and new methods of spectral estimation are investigated. Techniques considered are conventional beamsteer, maximum likelihood, maximum entropy and principle components. These techniques are evaluated using both synthetic data and real seismic data from the TFO extended short-period array.			

TA

14. KEY WORDS	LINK A		LINK B		LINK C	
	ROLE	WT	ROLE	WT	ROLE	WT
Array Processing						
Spectral Estimation						
Beamsteer						
Maximum Likelihood						
Maximum Entropy						
Principle Components						
Eigenvalue						
Eigenvector						
<i>Ih</i>						



APPROVED FOR PUBLIC RELEASE; DISTRIBUTION UNLIMITED

AFTAC Project No. VT/1705

RESOLUTION AND STABILITY OF WAVENUMBER  
SPECTRAL ESTIMATES

SPECIAL REPORT NO. 2  
EXTENDED ARRAY EVALUATION PROGRAM

Prepared by Aaron H. Booker and Chung-yen Ong

T. W. Harley, Program Manager  
Area Code 703, 836-3882 Ext. 300

TEXAS INSTRUMENTS INCORPORATED  
Services Group  
P. O. Box 5621  
Dallas, Texas 75222

Contract No. F33657-71-C-0843  
Amount of Contract: \$511,580  
Beginning 1 April 1971  
Ending 31 March 1972

Prepared for  
AIR FORCE TECHNICAL APPLICATIONS CENTER  
Washington, D. C. 20333

Sponsored by  
ADVANCED RESEARCH PROJECTS AGENCY  
Nuclear Monitoring Research Office  
ARPA Order No. 1714  
ARPA Program Code No. 1F10

30 April 1972

Acknowledgement: This research was supported by the Advanced Research Projects Agency, Nuclear Monitoring Research Office, under Project VELA-UNIFORM, and accomplished under the technical direction of the Air Force Technical Applications Center under Contract No. F33657-71-C-0843.

II

## ABSTRACT

The relative resolution and stability of conventional and new methods of spectral estimation are investigated. Techniques considered are conventional beamsteer, maximum likelihood, maximum entropy and principle components. These techniques are evaluated using both synthetic data and real seismic data from the TFO extended short-period array.

Neither the Advanced Research Projects Agency nor the Air Force Technical Applications Center will be responsible for information contained herein which has been supplied by other organizations or contractors, and this document is subject to later revision as may be necessary. The views and conclusions presented are those of the authors and should not be interpreted as necessarily representing the official policies, either expressed or implied, of the Advanced Research Projects Agency, the Air Force Technical Applications Center, or the US Government.

## TABLE OF CONTENTS

SECTION	TITLE	PAGE
	ABSTRACT	iii
I.	INTRODUCTION	I-1
II.	MATHEMATICAL DESCRIPTION OF TECHNIQUES AND RESOLUTION RESULTS	II-1
	A. GENERAL	II-1
	B. MATHEMATICAL DESCRIPTION OF THE TECHNIQUES	II-2
	C. COMPARATIVE RESOLUTION CAP- ABILITIES FOR THE SYNTHETIC DATA	II-4
III.	STABILITY RESULTS	III-1
IV.	TFO EIGENSPECTRA ANALYSIS	IV-1
	A. REVIEW OF PREVIOUS ANALYSIS	IV-1
	B. EIGENSPECTRA COMPUTATIONS	IV-1
	C. WAVENUMBER ANALYSIS OF EIGENVECTORS	IV-5
V.	CONCLUSIONS	V-1
VI.	REFERENCES	VI-1

## LIST OF FIGURES

FIGURE	TITLE	PAGE
II-1	SPECTRAL COMPARISON – SEVEN SIGNALS	II-6
II-2	SIDELOBE OF MAXIMUM ENTROPY SPECTRUM	II-7
II-3	EIGENSPECTRA OF SEVEN SIGNALS	II-9
II-4	EFFECT OF ISOTROPIC NOISE ON SPECTRA	II-11
II-5	EFFECT OF ISOTROPIC NOISE ON EIGEN- SPECTRA	II-12
II-6a	SPECTRA FOR SIGNALS NEAR IN AZIMUTH	II-13
II-6b	EIGENSPECTRA FOR SIGNALS NEAR IN AZIMUTH	II-14
III-1a	STABILITY OF SPECTRAL ESTIMATES, M=40	III-3
III-1b	STABILITY OF SPECTRAL ESTIMATES, M=40	III-4
III-1c	STABILITY OF SPECTRAL ESTIMATES, M=40	III-5
III-2	STABILITY OF SPECTRAL ESTIMATES, M=19	III-7
III-3	STABILITY OF EIGENSPECTRA	III-9
IV-1	TFO WAVENUMBER SPECTRUM AT LOW FREQUENCY (.12 Hz)	IV-2
IV-2	TFO WAVENUMBER SPECTRA AT HIGH FREQUENCY	IV-3
IV-3	TFO WAVENUMBER SPECTRUM – COMPARISON	IV-4
IV-4	TFO EIGENSPECTRUM 1	IV-6
IV-5	TFO EIGENSPECTRA 2, 3	IV-8
IV-6	TFO EIGENSPECTRA 4, 5	IV-9
IV-7	TFO WAVENUMBER SPECTRUM AT 0.33 Hz	IV-10
IV-8	TFO EIGENSPECTRA 6, 7, 8	IV-11
IV-9	TFO EIGENSPECTRUM 9	IV-12

## LIST OF TABLES

TABLE	TITLE	PAGE
II-1	SIGNAL MODELS FOR SPECTRAL EVALUATION	II-4
II-2	SIGNAL MODELS SELECTED FOR NON- ORTHOGONALITY	II-8
II-3	SIGNAL OF NEAR STRENGTH AND AZIMUTH	II-15
III-1	FIRST SIGNAL MODEL FOR STABILITY STUDIES	III-2
III-2	SECOND SIGNAL MODEL FOR STABILITY STUDIES	III-6
IV-1	NUMBER OF ITERATIONS AND RESULTING EIGENVALUE	IV-5

## SECTION I

### INTRODUCTION

The goal of this research is to investigate the relative resolution and stability of conventional and new methods of array processing or spectral estimation. Resolution as intended here will mean the directivity of the processing technique or the ability to differentiate two signals from almost the same direction. Also, we will investigate resolution from the point of view of the technique's ability to detect weak signals, i. e., the relative noise threshold of the techniques. These questions will be studied with true covariance matrices corresponding to a fixed number of plane wave signals plus noise. Stability is investigated by generating random column vectors  $V_i$ ,  $i=1, \dots, N$  from the covariance matrix  $\Omega$  and applying the techniques to the conventional estimate  $\hat{\Omega} = N^{-1} \sum_i V_i V_i^H$  of the covariance matrix, where  $H$  denotes conjugate transpose.

Two simplifications of the general problem have been made so that the computations become reasonable. First, we will conduct the analysis at a given frequency so that the matrix dimension is  $C$  by  $C$  where  $C$  is the number of sensors. Second, computation for the maximum entropy spectrum is greatly simplified by using a line array of equally spaced sensors, i. e., we avoid iterative methods for spectral estimation.

The techniques to be considered are conventional beamsteer BS, maximum-likelihood (unbiased minimum mean square error) ML, maximum entropy (K-Line or Burg technique), and principal components or eigenvalue analysis. Exact mathematical description of these techniques will be given in the following section.

The method of principal components differs somewhat in philosophy from the other techniques and it is not directly a method for spectral estimation

or array processing. Justification for its inclusion lies in its complete invariance to random noise and the tendency to isolate plane wave signals on eigenvectors ordered by signal strength. The procedure is to compute the eigenvectors and then compute the eigenvector response function (or eigenspectra), which is the absolute square value of the dot product of the eigenvector and a "look direction" vector. The direction at the maximum of the successive eigenspectra will be shown empirically to correspond to the directions of the plane wave signals specified in the covariance matrix. Mathematically  $\Omega Z = \lambda Z$  must be satisfied, where  $Z$ , and  $\lambda$  are an eigenvector and eigenvalue of  $\Omega$ . Thus  $(\Omega + \beta I) Z = (\lambda + \beta) Z$  for any constant  $\beta$ , so that the eigenvectors of  $\Omega$  are also the eigenvectors of  $\Omega + \beta I$  and the technique is therefore expected to be insensitive to random noise.

There has been considerable previous theoretical treatment of the principal components method but very little actual application of the technique to array processing. The classical multivariate statistics approach is treated by Anderson (1958) and the interpretation of these results in terms of multiple stationary time series is discussed by N. R. Goodman (1967). The actual stimulation for our consideration of principal components in the present effort came from a paper by N. L. Owsley (1971) where he suggested that plane wave signals tend to be isolated on individual eigenvectors and ordered according to strength.

SECTION II  
MATHEMATICAL DESCRIPTION OF TECHNIQUES AND  
RESOLUTION RESULTS

A. GENERAL

A synthetic or theoretical cross-power matrix was computed and used to evaluate the following four types of spectra estimates:

- Beamsteer (BS)
- Maximum-Likelihood (ML)
- Markoff or K-Line (MK)
- Eigenvalue-Vector (EG)

The cross-power matrices,  $\Omega$  were generated from special signal vectors,  $s_j$ , where  $j = 1, 2, \dots, N$ , according to the equation:

$$\Omega = \sum_{j=1}^N \alpha_j s_j s_j^H + \beta I$$

where the  $\alpha_j$ 's and  $\beta$  are the relative weights for the individual signals and random noise component respectively, and  $H$  consists of the operation of transposition and conjugation.

The elements of the signal vector are defined as:

$$s_j(\ell) = e^{-i2\pi f \Delta t_j(\ell)} \quad , \quad \ell = 1, 2, \dots, C$$

where  $C$  is the number of elements or array sensors to be used in the evaluation,  $f$  is frequency, and  $\Delta t_j(\ell)$  is the time delay for the  $\ell^{\text{th}}$  channel in the  $j^{\text{th}}$  look direction. The array can be three-dimensional,  $(X, Y, Z)$ . The signal vectors are specified by an azimuth angle (clockwise direction from positive Y-ordinate in X-Y plane), elevation angle (angle of incidence), and a propagation velocity.

Power,  $P$ , is computed for a matrix generated at a selected frequency as a function of the "look direction" (that is, the direction having an azimuth angle of  $\theta$ ) for each of the previously listed techniques. The "look direction" vector,  $S(\theta)$  is defined similarly to the signal vector except the angle of elevation is assumed to be zero. Starting with  $\theta=0$  and increasing  $\theta$  in even increments until  $\theta=2\pi$  provides a complete azimuth-power spectrum.

## B. MATHEMATICAL DESCRIPTION OF THE TECHNIQUES

The following is a brief description of the procedure used to calculate these spectra.

### 1. Beamsteer Spectra, $P_{BS}(\theta)$

The beamsteer spectra are the response of the beamed (in the "look direction",  $\theta$ ) array to the data matrix  $\Omega$ . Effectively the beamed array has the response of a filter vector  $b$  defined as:

$$b = S(\theta)/C$$

so that

$$P_{BS}(\theta) = b^H \Omega b$$

By the definition of  $\Omega$  the spectra are actually computed by the equation:

$$P_{BS}(\theta) = \sum_{j=1}^N \alpha_j \left| b^H s_j \right|^2 + \beta/C$$

### 2. Maximum-likelihood, $P_{ML}(\theta)$

The maximum-likelihood filter  $M(\theta)$ , is defined by

$$M(\theta) = \Omega^{-1} S / (S^H \Omega^{-1} S)$$

Therefore the maximum-likelihood spectrum is given by:

$$P_{ML}(\theta) = M(\theta)^H \Omega M(\theta) = 1 / [S(\theta)^H \Omega^{-1} S(\theta)]$$

### 3. Maximum Entropy, $P_{MK}(\theta)$

The technique as programmed is applicable only to an array consisting of elements with equal spacing  $\Delta x$  along a single line or several parallel lines. In the case of several lines of sensors the cross-power matrix for each line is stacked to form a single matrix  $\Omega_K$  dimensioned by the size of the largest individual line matrix.

The inverse of  $\Omega_K$  is computed and prediction error filters,  $A_l$ , are determined. The azimuthal power spectra is then computed according to the following:

$$P_{MK}(\theta) = 2 p \Delta x \left| \sum_{l=1}^C A_l e^{-i2\pi k \Delta x} \right|^{-2}$$

where  $p$  is the prediction error and  $k$  is the wave number, which is given by:

$$k = f \cos \theta / V.$$

where  $V$  is the velocity of propagation.

### 4. Eigenspectra, $P_{EG}(\theta)$

The matrix,  $\Omega$ , can be represented as

$$\Omega = \sum_{l=1}^C \lambda_l g_l g_l^H$$

where  $\lambda_l$  and  $g_l$  are the eigenvalues and eigenvectors respectively of the matrix  $\Omega$ . Having developed the matrix,  $\Omega$ , from the specified signal vectors, the

eigenvalues and eigenvectors are now extracted from  $\Omega$  and compared to the original weighting values  $\alpha_j$  and signal vectors  $s_j$ . The response of the eigenvectors associated with the eigenvalues are computed as the eigenspectra,  $P_{EG_l}$ , where

$$P_{EG_l}(\theta) = \left| g_l^H S(\theta) \right|^2, \quad l = 1, \dots, C.$$

The  $\lambda_l$ 's are arranged in decreasing order of magnitude.

### C. COMPARATIVE RESOLUTION CAPABILITIES FOR THE SYNTHETIC DATA

The resolution and accuracy of each of the spectral estimates were evaluated from a cross-power matrix at 3.0 Hz. developed from seven signal vectors and 1 per cent random noise. The specifications for the seven signals are presented in Table II-1; note that the signals are progressively smaller and that Signal 7 is 50 dB down from Signal 1.

TABLE II-1  
SIGNAL MODELS FOR SPECTRAL EVALUATION

Signal Number	Velocity	Azimuth	Elevation	Weighting	Relative Power (dB)
1	10 km/sec	0.0	0.0	10,000	0.0
2	"	40.0	0.0	1,000	-10.0
3	"	320.0	0.0	.100	-20.0
4	"	340.0	0.0	.0100	-30.0
5	"	300.0	0.0	.0050	-33.0
6	"	20.0	0.0	.0010	-40.0
7	"	60.0	0.0	.0001	-50.0

The array consisted of 20 equally spaced elements at 1 km intervals along the X-ordinate. Thus a value of  $\theta = 0$  corresponds to a look direction perpendicular to the array.

The spectral estimates obtained by the BS, ML and MK methods are shown in Figure II-1. The exact location of the signals are marked by vertical lines at the top of the figure. The MK spectrum is plotted by scaling its maximum value to that of the ML spectrum. Azimuth is plotted over  $360^\circ$  for the line array so the interval  $90^\circ$  to  $270^\circ$  is the alias of the remainder of the plot. An analysis of the figure shows that only the first two signals (1 and 2) are resolved by the BS spectra. Signals 1-5 were resolved by both the ML and MK spectra, with the MK spectra exhibiting much sharper and stronger peaks than the ML spectra.

None of the three methods were able to resolve the weak signal 6 which was positioned between the two strong signals 1 and 2. However, an even weaker signal (No. 7) seems to have been resolved by the MK estimate. To determine if signal 7 was being resolved or if the peak is just a sidelobe effect, another spectral computation run was made in which signal 7 was moved further away from signal 2. As shown in Figure II-2 the peak did not move with the signal location indicating sidelobe effects and the inability of all three techniques to resolve this signal energy.

In the second run, the weighting of signal 6 was increased by 7 dB, leaving its level 33 dB down from the adjacent signal 1. In this case (Figure II-2) both the ML and MK spectra evidently resolved the signal energy. At the same time, signal 5 was decreased by 7 dB to 40 dB down from signal 1. Here the MK spectra still resolved the energy but the ML spectra tends to lose the energy peak.

EG spectra were computed from the cross-power matrices on which the previous three techniques were evaluated. For the first case, seven eigenvectors were extracted from the matrix and spectral estimates made from each. Arranging the EG spectra in order based on the decreasing value of the eigenvalues, a one-to-one correspondence of the dominating peak in each of the spectra

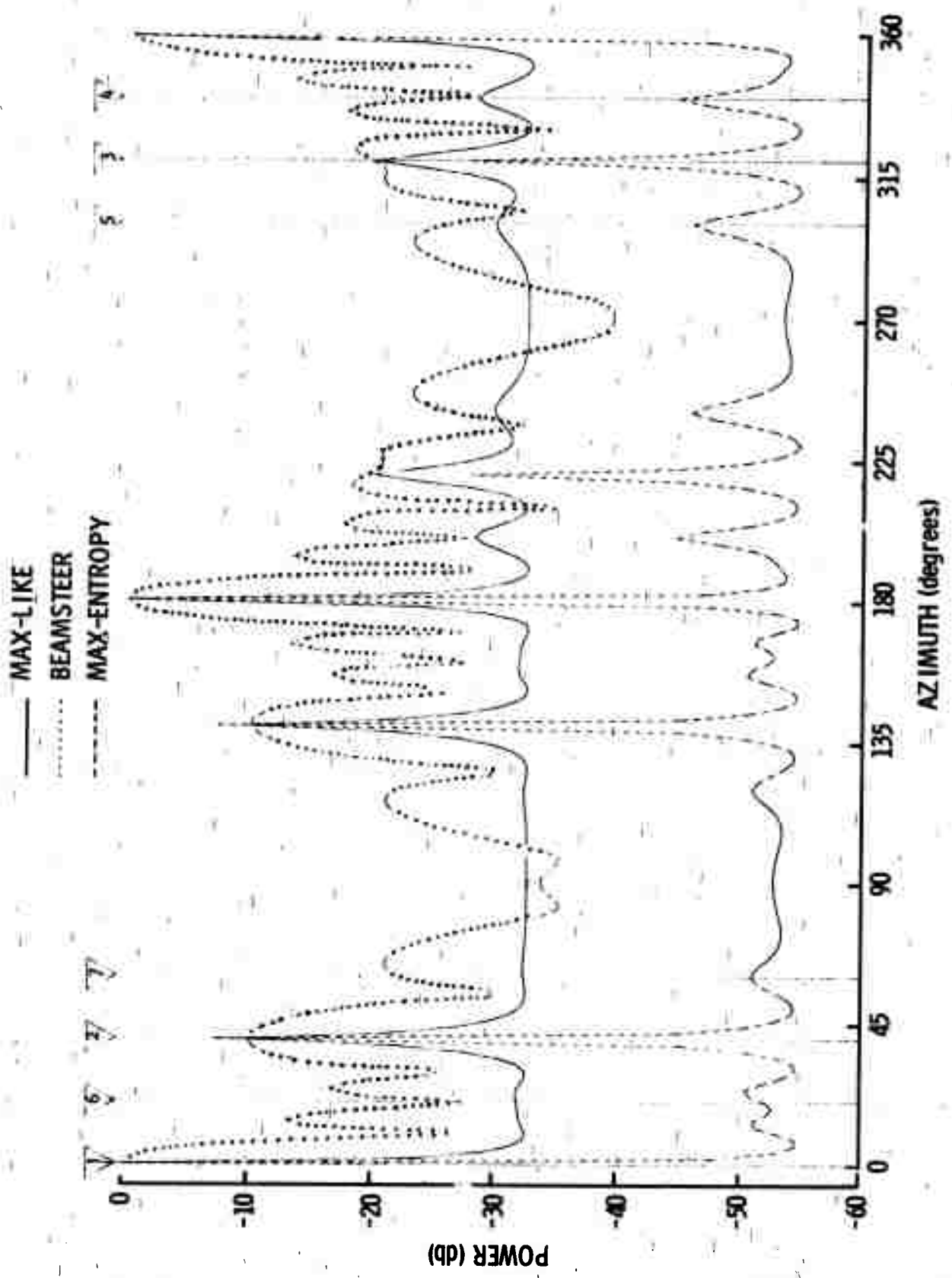


Figure II-1. Spectral Comparison - Seven Signals

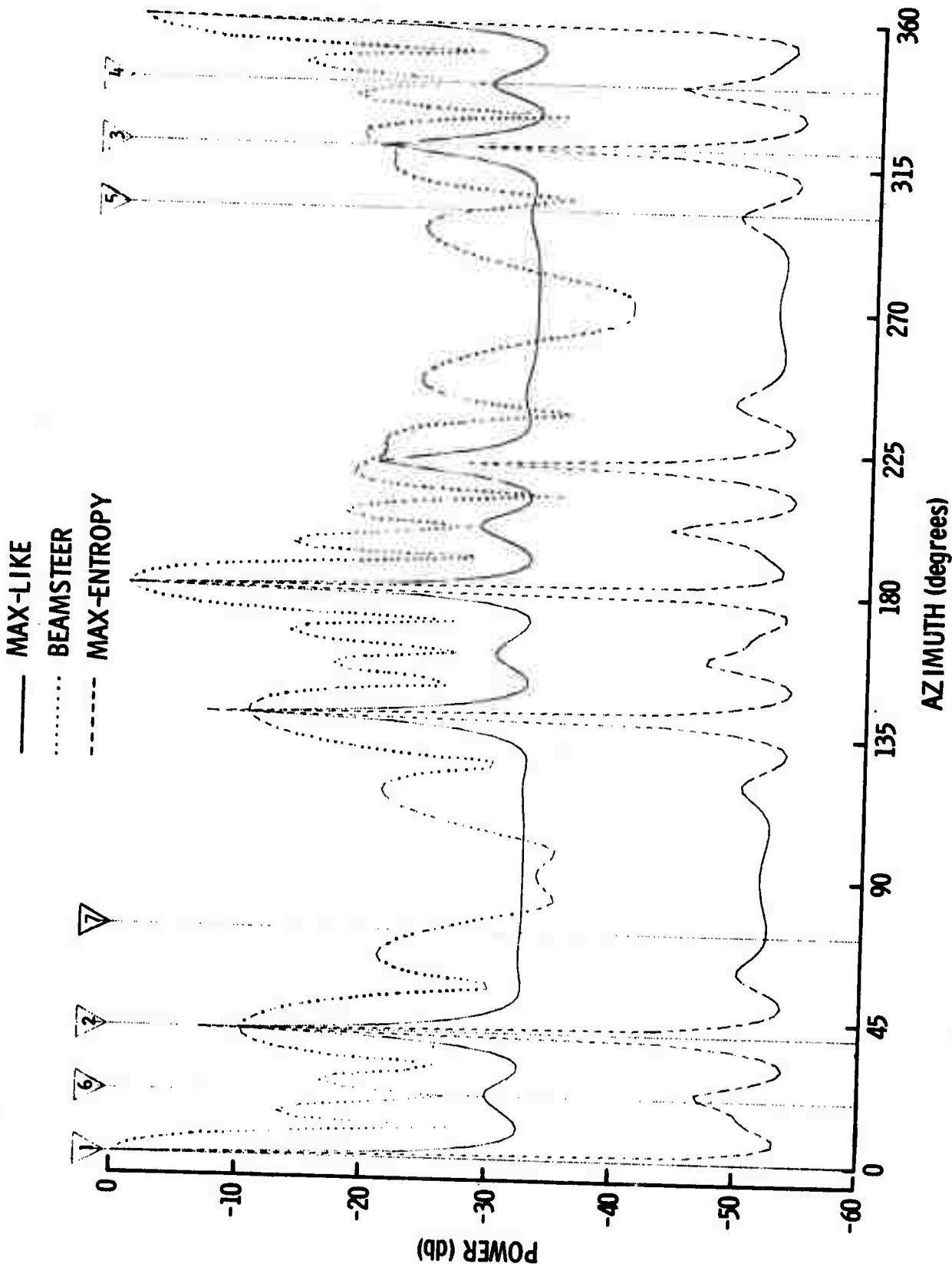


Figure II-2. Side Lobe of Maximum Entropy Spectrum

to the signals 1 through 7 was made. (Figure II-3). The resolution of signals 6 and 7, which were previously unresolved by the other techniques, is extremely encouraging. Similarly, the EG spectra from the second run, resolved all of the signals. Spectra from the additional eighth and ninth eigenvectors computed in this run showed many lobes within 6 dB of each other indicating that no significant signal energy remained in the matrix after the extraction of the first seven eigenvectors. (We have chosen to require the EG spectra to have a peak 6 dB above the general sidelobe level before a signal component is "identified".)

To further test the EG spectra method, a set of signals were chosen in which several pairs of the signals were picked to be highly non-orthogonal (i. e., the direction of the second signal of the pair was in the direction of the maximum sidelobe of the first signal).

The signal models in this case are listed in Table II-2.

TABLE II-2  
SIGNAL MODELS SELECTED FOR NON-ORTHOGONALITY

Signal Number	Velocity	Azimuth	Elevation	Weighting	Relative Power (db)
1	10 km/sec.	0.0	0.0	10.0000	0.0
2	"	14.0	0.0	1.0000	-10.0
3	"	29.0	0.0	.1000	-20.0
4	"	319.0	0.0	.0100	-30.0
5	"	46.0	0.0	.0050	-33.0
6	"	305.0	0.0	.0010	-40.0
7	"	73.0	0.0	.0001	-50.0

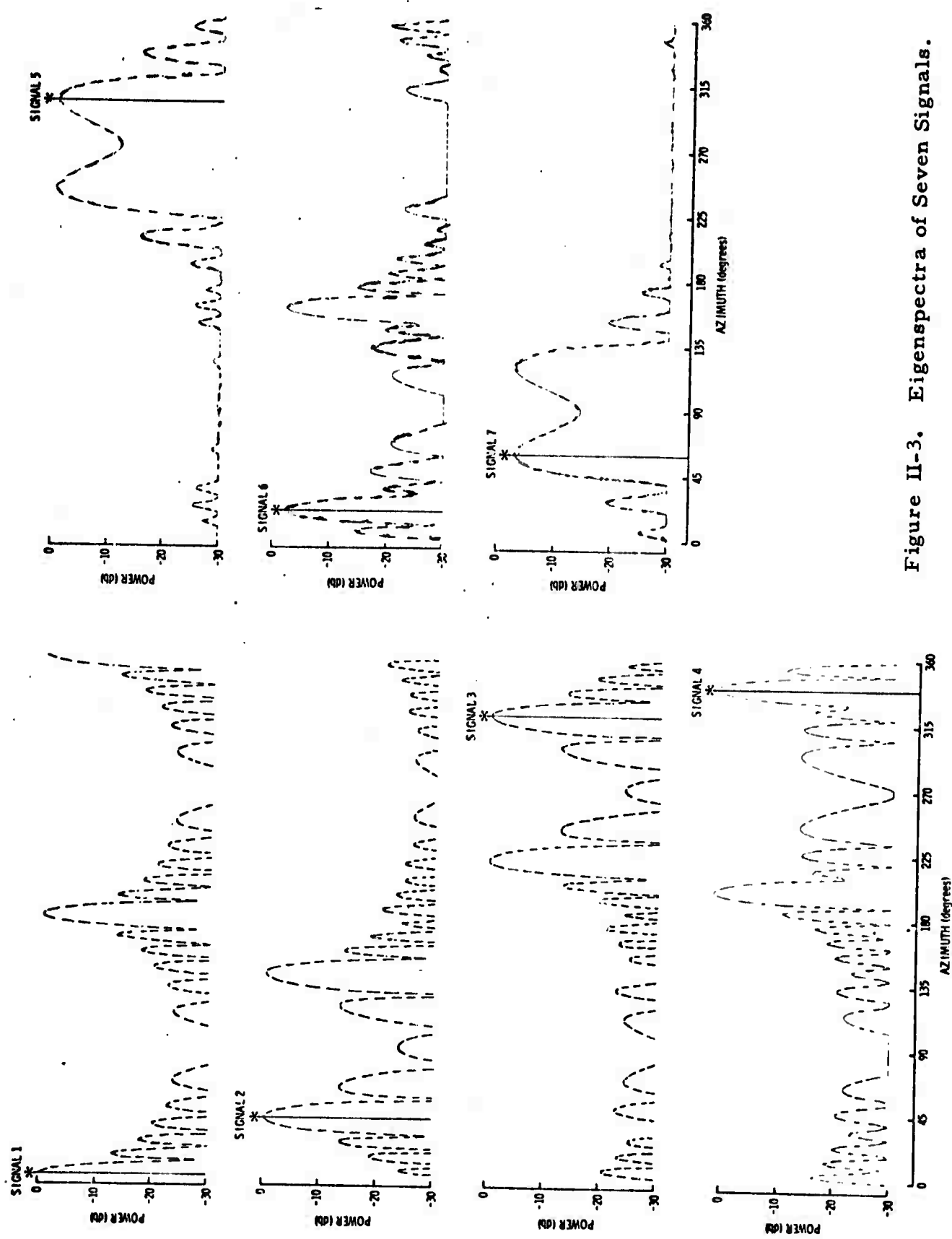


Figure II-3. Eigenspectra of Seven Signals.

Results from these signal models were similar to those of the previous two runs. That is, the BS spectra could resolve only the first two signals, ML and MK spectra resolved the first 5 signals, and the EG spectra resolved all seven signals.

The effects of isotropic noise on the ML, MK and EG spectral estimates was evaluated using the signals presented in Table II-2, (Figures II-4 and II-5). The previously discussed run did not contain any isotropic noise. The addition of 1% isotropic noise had a negligible effect on the EG spectra. The most significant effect occurred in the ML spectra where the "whole" noise level increased 3 to 5 dB, almost obscuring signal 5.

The addition of 10 percent isotropic noise prevented both the ML and MK spectral estimates from resolving signals 4 and 5. However, the EG spectra still resolved all seven of the signals, although the azimuth of the weakest signal was biased (Figure II-5). The eigenspectra for the stronger signals (1-5) were not significantly effected by the isotropic noise. The sidelobes of the eigenspectra corresponding to the weaker signals increased approximately 5 dB due to the isotropic noise, however the signal peaks were still predominant enough to allow detection of signals.

Two final data matrices were constructed using the parameters in Table II-3 in order to investigate signals extremely close in azimuth and signals of near equal strength. The signal vectors were not normalized in the program so the approximate eigenvalues (assuming independence of the input signal vectors) are 20 times the input signal strength. Calculated eigenvalues are shown in the table and are similar to the approximate values, given in parentheses.

Signals near in azimuth were grouped into azimuthal pairs separated by only a few degrees and were selected so that all the pairs were in the main lobe of the beamsteer response pattern. Spectra obtained from the BS, ML and MK techniques are shown in Figure II-6a, for the EG technique in Figure II-6b. The

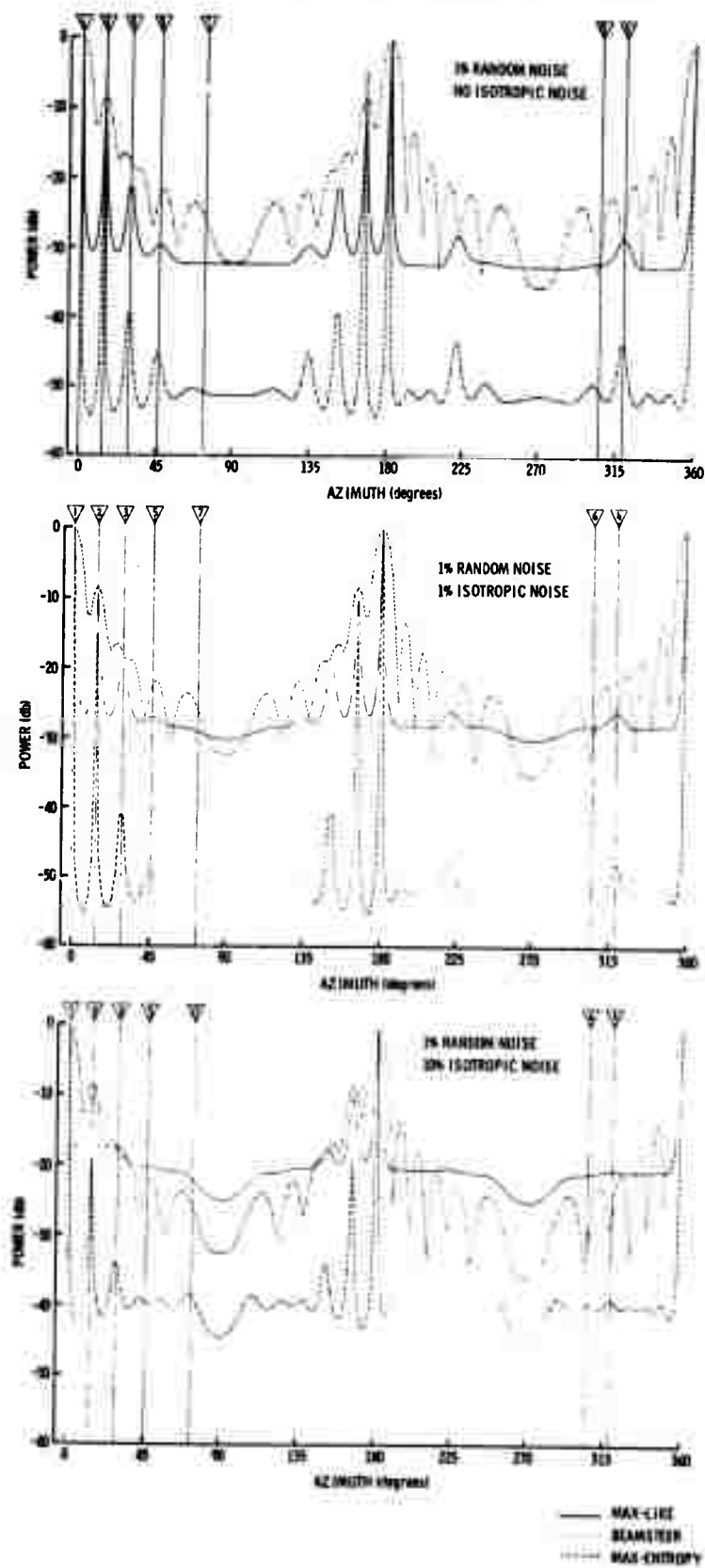


Figure II-4. Effect of Isotropic Noise on Spectra

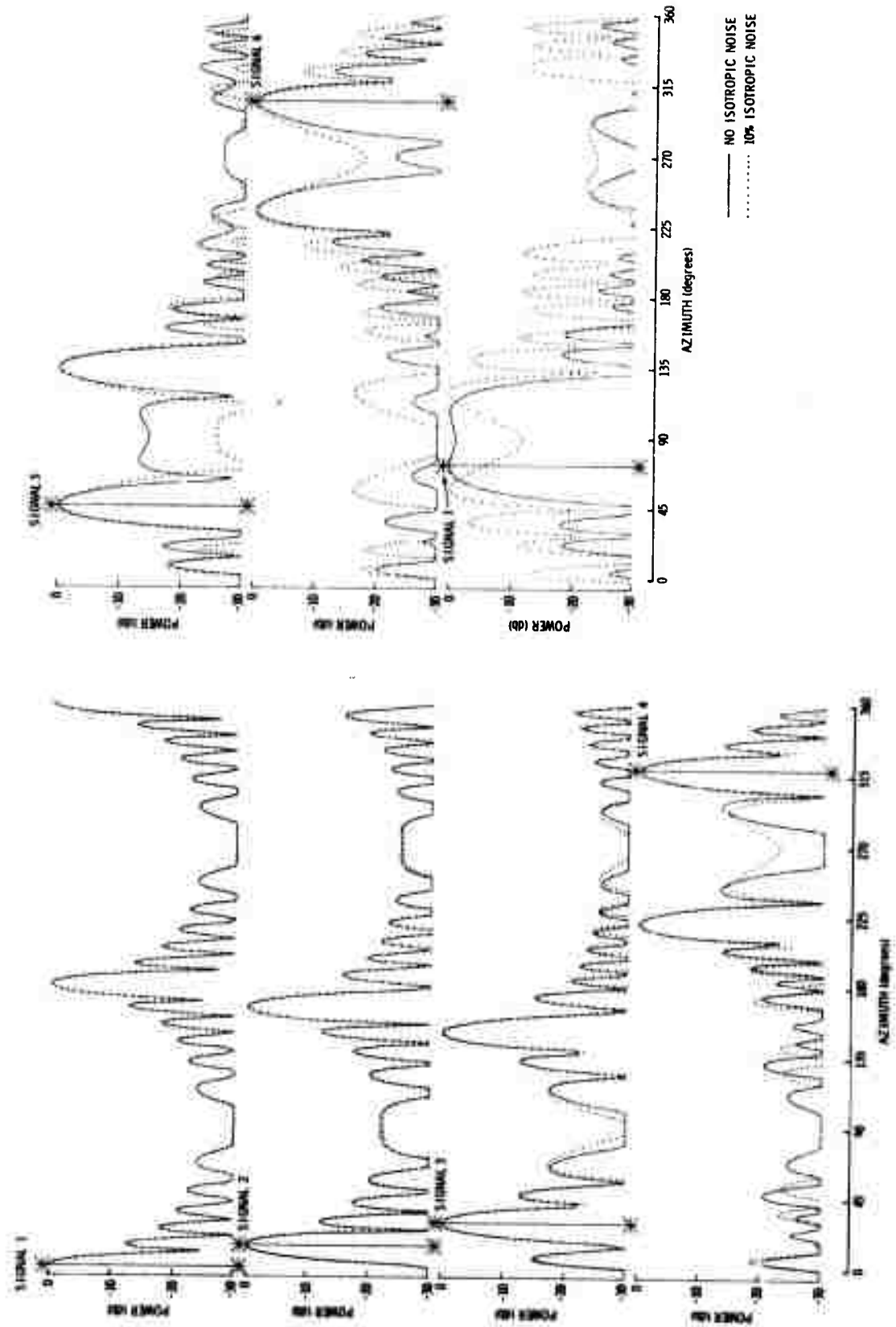


Figure II-5. Effect of Isotropic Noise on Eigenspectra

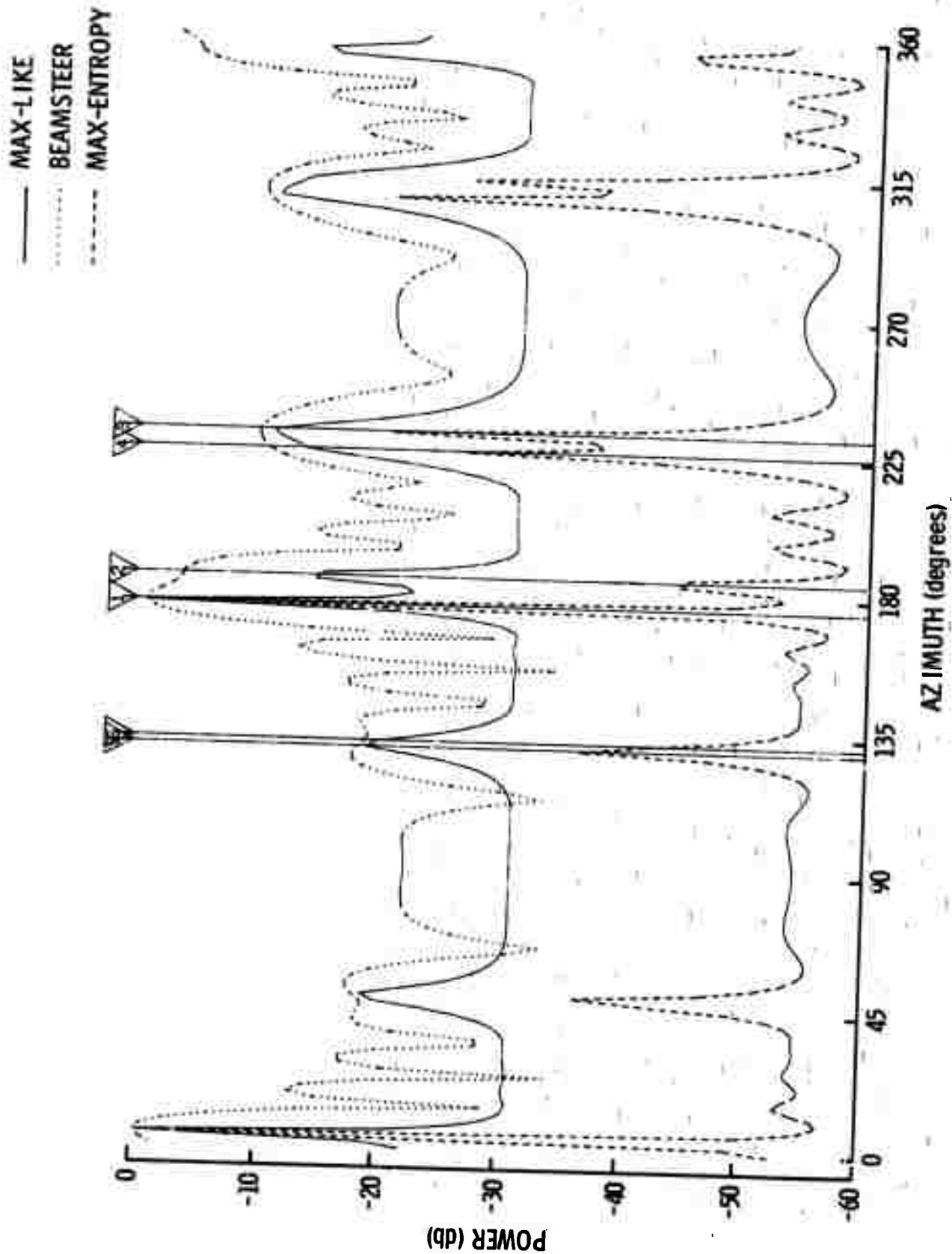


Figure II-6a. Spectra For Signals Near In Azimuth

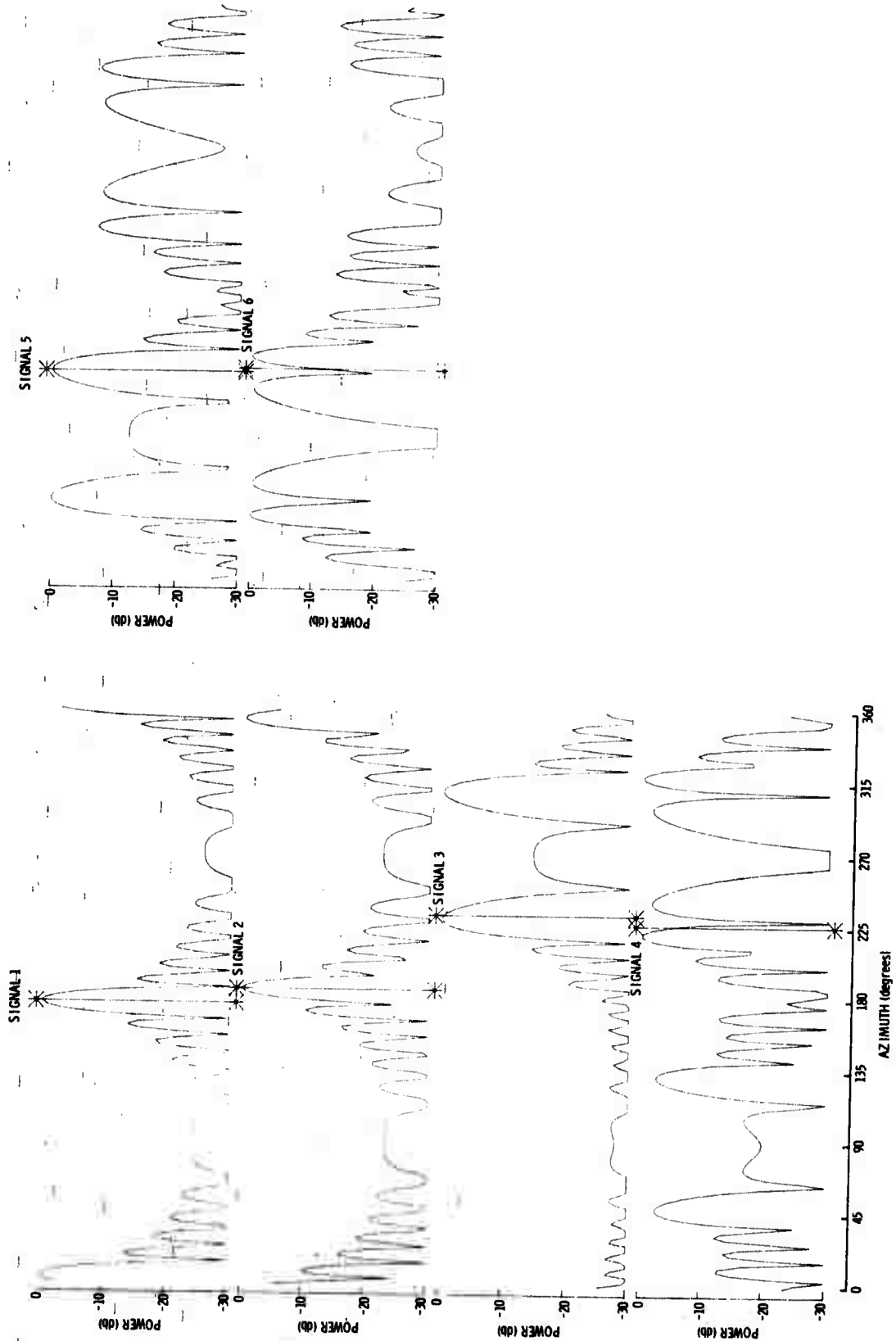


Figure II-6b. Eigenspectra For Signals Near In Azimuth

TABLE II-3  
SIGNAL OF NEAR STRENGTH AND AZIMUTH

Signal Number	Near Azimuth			Near Strength			
	Azimuth	Strength	Eigenvalue	Azimuth	Strength	Eigenvalue	
1	176	10	(200)	0	10	(200)	209.6
2	185	5	(100)	14	5	(100)	98.8
3	232	1	(20)	29	3	(60)	56.3
4	226	.5	(10)	319	2	(40)	40.2
5	130	.1	(2)	46	1.5	(30)	30.0
6	132	.05	(1)	305	1.2	(24)	23.7
7				73	1.1	(22)	19.0

MK method has the best capability because it resolves signals 3 and 4 as well as signals 1 and 2. The ML and EG techniques resolve signals 1 and 2 only, the BS technique does not resolve any pair.

Results for the near equal strength data were the same as those obtained previously and the figures are not shown.

SECTION III  
STABILITY RESULTS

The spectral estimation techniques evaluated for resolution in the preceding section on the "true" matrix for the set of specified signal vectors as defined by:

$$\Omega = \sum_{j=1}^N \alpha_j s_j s_j^H + \beta I$$

were also evaluated for stability on an "estimate",  $\hat{\Omega}$ , of the true matrix  $\Omega$  defined as

$$\hat{\Omega}_{i+1} = \gamma \hat{\Omega}_i + (1 - \gamma) X_i X_i^H$$

where  $\gamma$  is an exponential decay factor and  $X_i$  is the  $i^{\text{th}}$  generated transform vector based on the set of specified signals. That is,

$$X_i = \sum_{j=1}^N \epsilon_j s_j + \beta^{1/2} \eta_i$$

where  $\epsilon_j$  is an independent scalar gaussian deviate such that  $E \left[ \epsilon_j \epsilon_j^* \right] = \alpha_j$  and  $\eta_i$  is a normally distributed random vector with zero mean and identity covariance.

An estimate of the matrix could be obtained by an average of  $L$  matrices, each generated from a transform vector,  $x_j$ , as previously defined. That is,

$$\hat{\Omega}_1 = \sum_{j=1}^L X_j X_j^H / L$$

The stability of the spectral estimation techniques will be a function of the decay factor,  $\gamma$ . The number  $M$  (equivalent to  $L$  for successive updates of  $\Omega_i$ ) is related to  $\gamma$  by the equation:

$$M = (1 + \gamma) / (1 - \gamma)$$

The first stability test run was conducted on an "estimated" matrix computed as outlined above from the set of three signals described in Table III-1, with  $\gamma = .95$  and the number of updates between spectral estimates  $M = 40$ .

TABLE III-1  
FIRST SIGNAL MODEL FOR STABILITY STUDIES

Signal Number	Velocity	Azimuth	Elevation	Weighting
1	10 km/sec	240.0	0.0	2
2	"	92.0	0.0	1
3	"	150.0	0.0	.5

Starting with an initial matrix generated from the average of 20 data vectors, a set of spectral estimations was made from the "estimated" matrix after 40, 80, and 120 updates. The spectra after 40, 80, and 120 updates are shown in Figures III-1a through III-1c with the BS, ML (which is plotted 28 dB down) and MK spectra at the top and the three EG spectra at the bottom. The MK spectra were developed from 5 point prediction filters thereby resulting in somewhat lower resolution than observed in the previous study. The stability of all estimation techniques is extremely good for this case, the three estimates (for a given technique) are virtually identical.

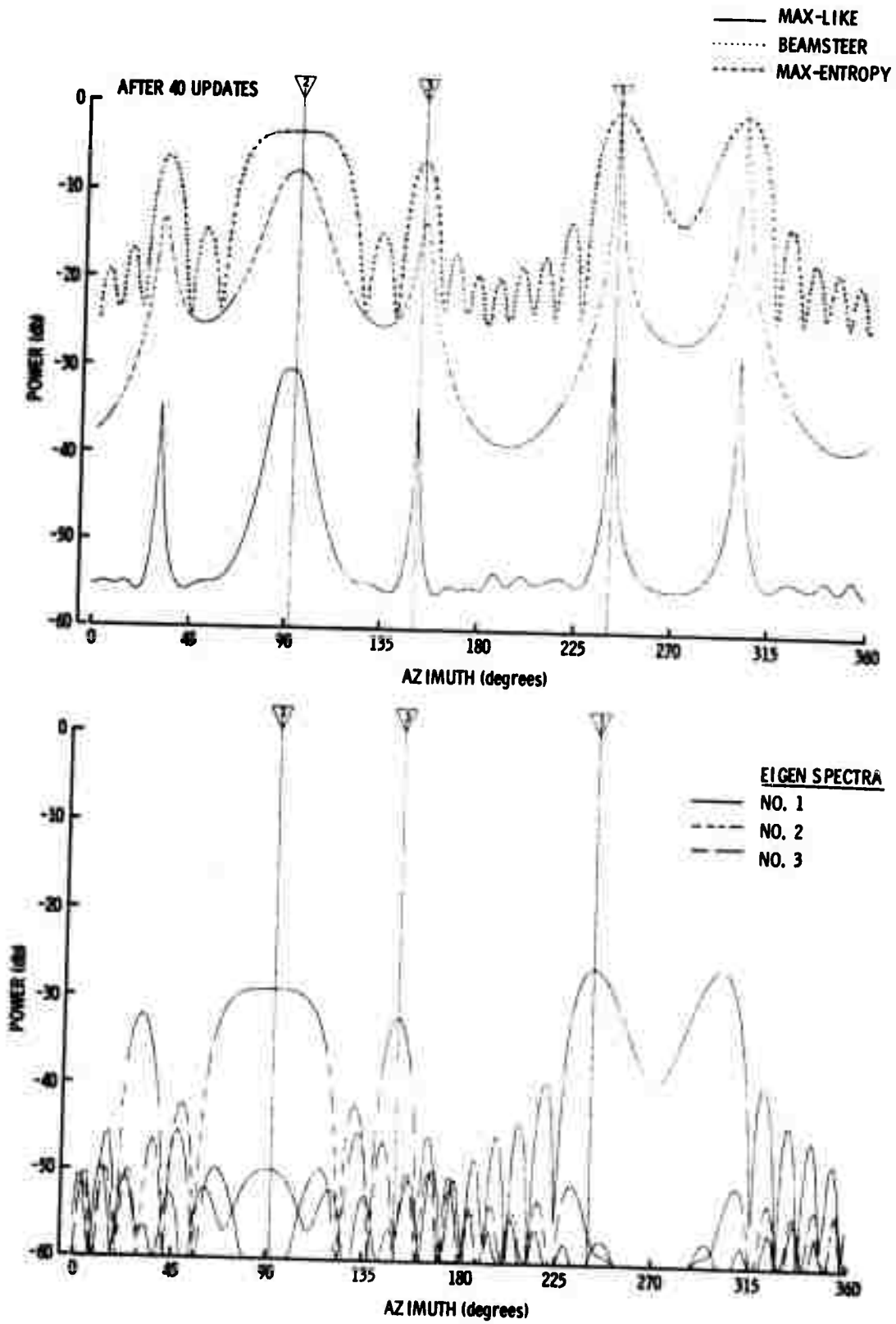


Figure III-1a. Stability of Spectral Estimates, M=40

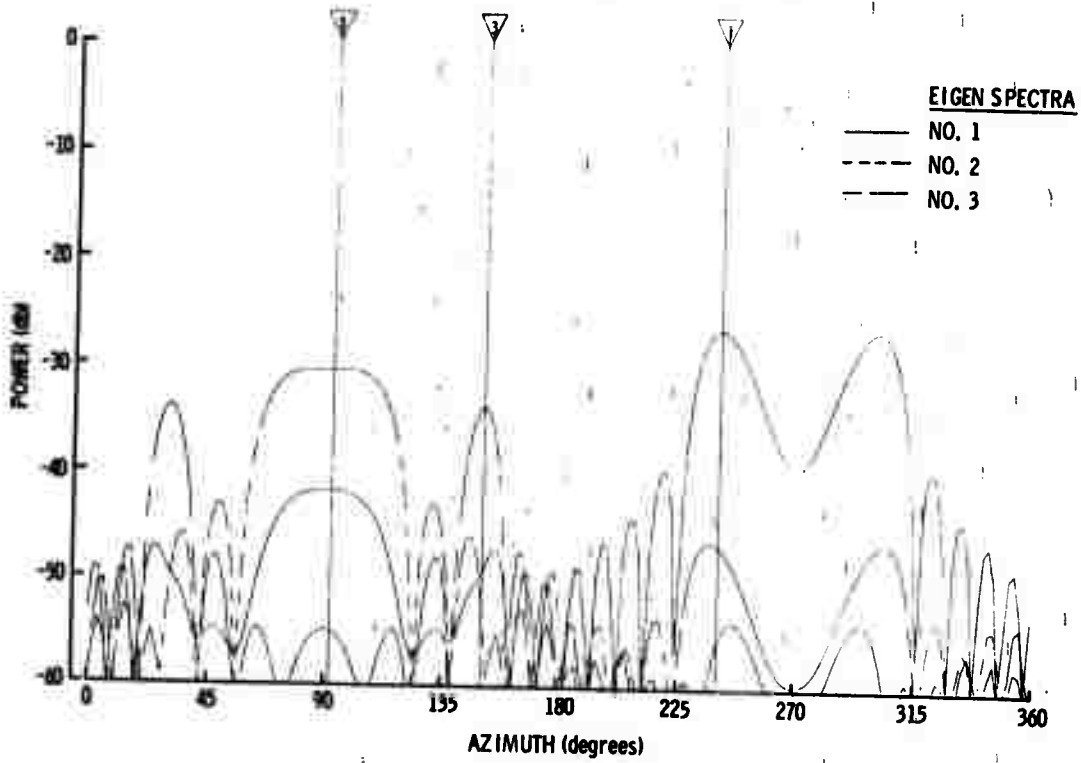
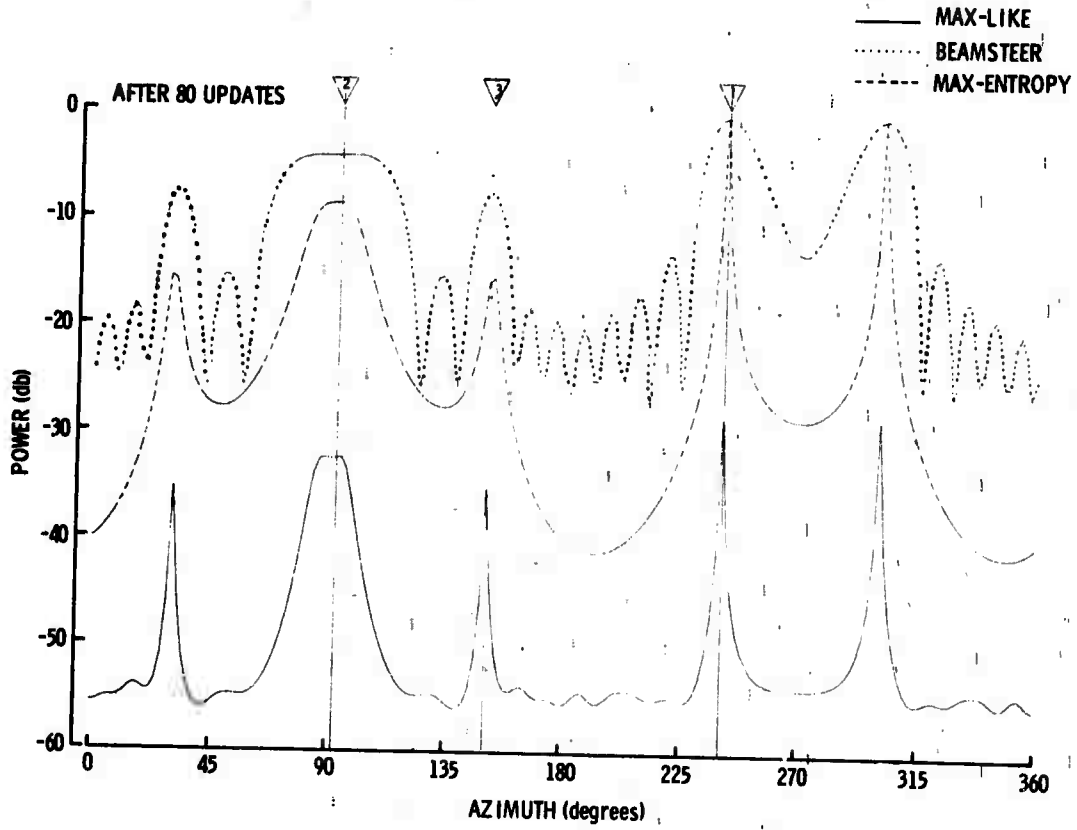


Figure III-1b. Stability of Spectral Estimates,  $M=40$

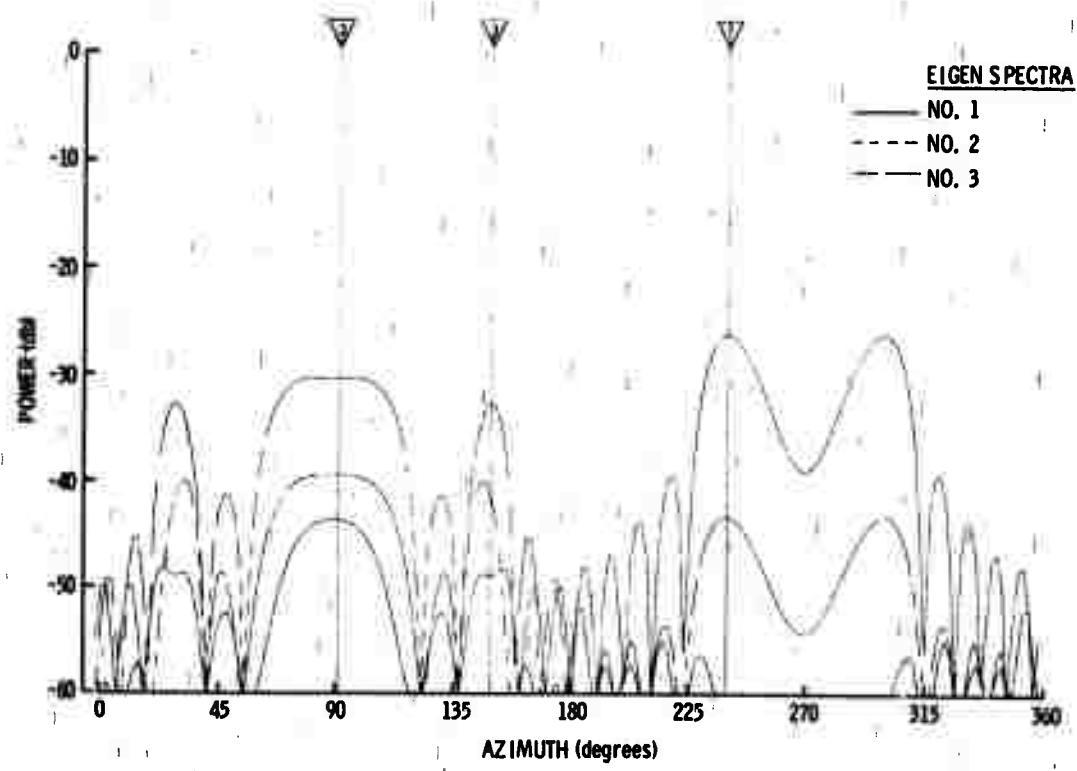
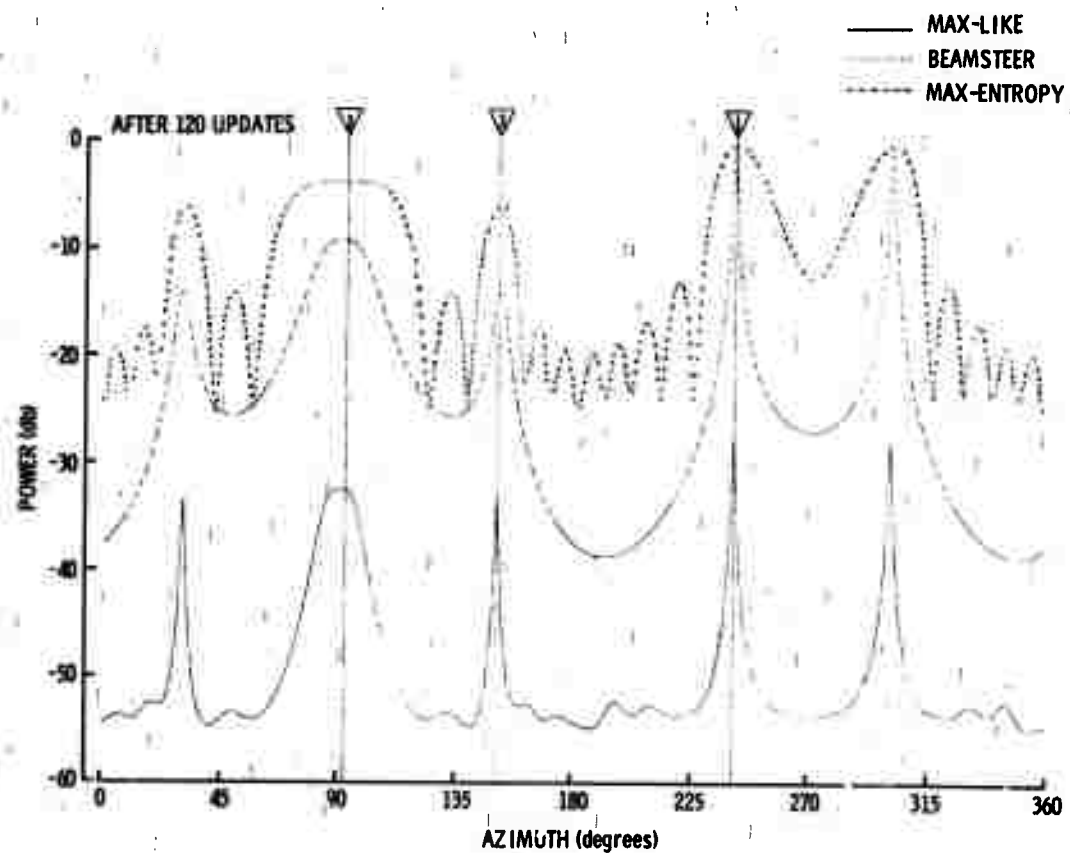


Figure III-1c. Stability of Spectral Estimates, M=40

A second case was run to further evaluate the stability of the estimation in which the decay rate was increased by lowering  $\gamma$  to .9 . Seven signal vectors as described in Table III-2 were used in this case. The number of updates, M, between successive spectra computations was 19.

TABLE III-2  
SECOND SIGNAL MODEL FOR STABILITY STUDIES

Signal Number	Velocity	Azimuth	Elevation	Weighting
1	10 km/sec	180.0	0.0	10.000
2	"	240.0	0.0	2.000
3	"	92.0	0.0	1.000
4	"	150.0	0.0	.500
5	"	120.0	0.0	.100
6	"	210.0	0.0	.010
7	"	270.0	0.0	.001

The ML and MK spectra computed after 19, 38, and 57 updates are presented in Figure III-2. For the MK spectra, a 10 point prediction error filter was used. The stability of the estimates for the signals 1 to 4 appear to be very good for all processes with one exception; the MK spectra was slightly unstable in the area of signal 3.

Signal 5 was resolved only by the ML estimate and the stability seems to be fair. Signal 6 was resolved by both the ML and MK estimates, however the MK line is rather unstable. The seventh signal was not resolved by any of the three techniques.

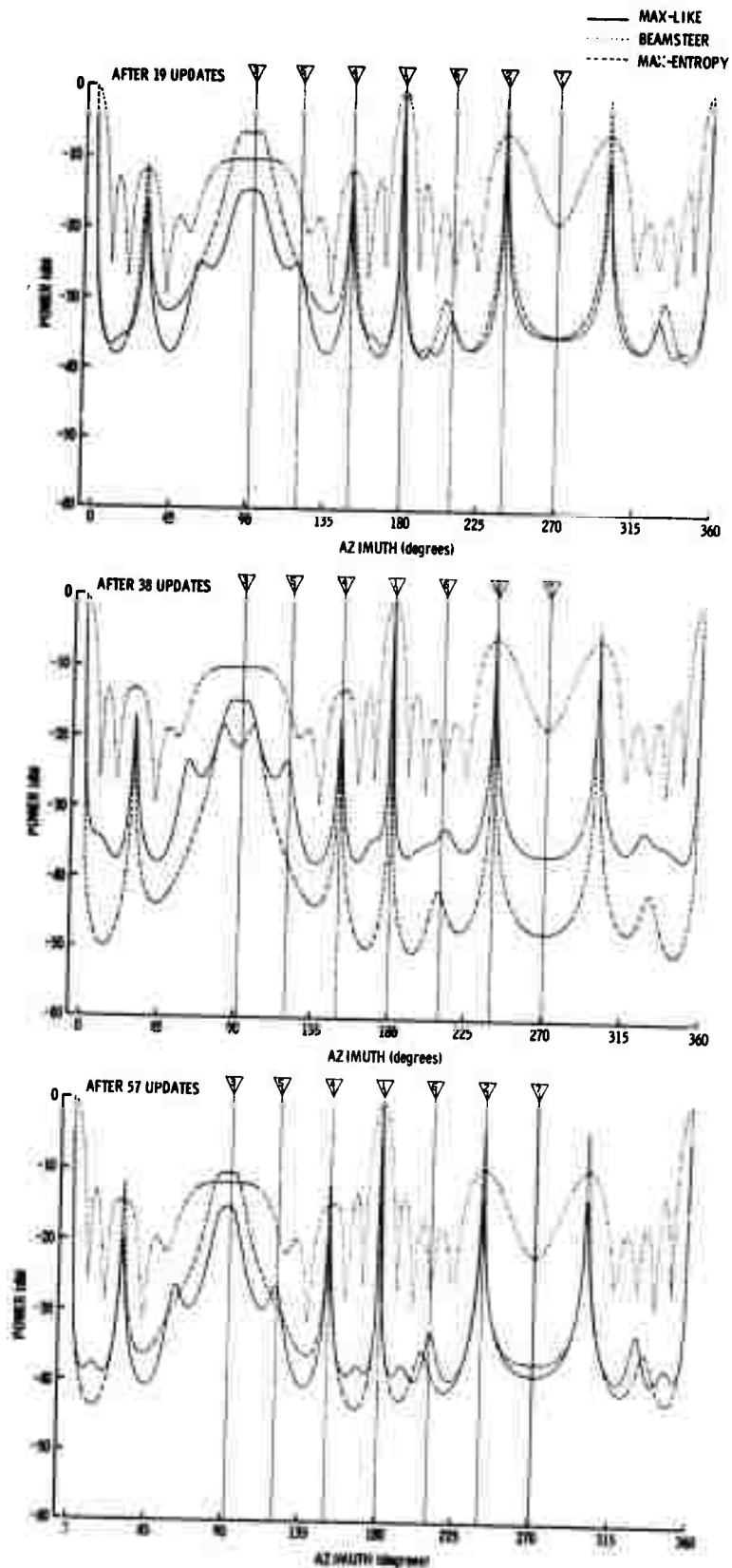


Figure III-2. Stability of Spectral Estimates, M=19

Similarly, EG spectra were computed for the "estimated" matrices (at the end of 19, 38, and 57 updates). The spectra computed from the first eight extracted eigenvectors of each matrix are shown in Figure III-3. The stability of the spectra in the area of the signal appears to be very good.

The first six signals are detectable in all sets of the EG spectra. Note that signals 2, 3, and 4, whose specified power levels relative to the strongest signal are -7, -10, and -13 dB respectively, appear to be somewhat mixed in the second, third, and fourth EG spectra. That is, spectrum No. 2 contains primarily signal 2 with an indication of signal 3 and spectrum No. 3 contains primarily signal 4 with an indication of both signals 2 and 3. However, because these "overlapped" signals are 6 dB or more below the "target" signal, it is still possible to unambiguously identify signal  $S_i$  from EG spectrum No.  $S_i$ .

Although spectrum No. 7 consistently peaked up at the location of signal 7, the signal would not have been detectable from the computed spectrum, because the sidelobes are as large as the actual peak. However, if spectrum No. 7 were averaged over time, that is after updates 19, 38, and 57, etc., signal 7 might be detectable because of the unstable nature of the spectra outside the area of signal 7 relative to the stability in that area.

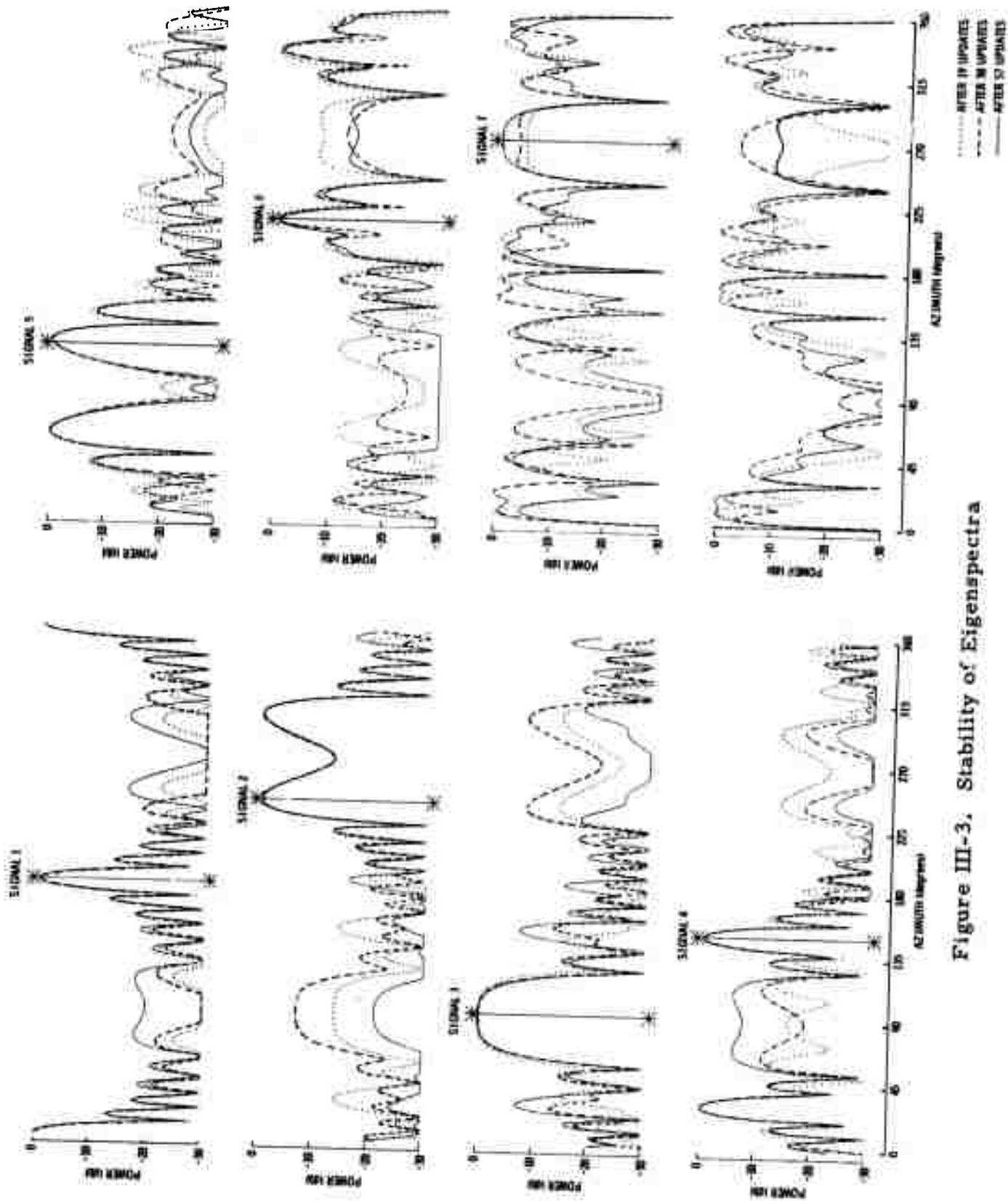


Figure III-3. Stability of Eigenspectra

## SECTION IV

### TFO EIGENSPECTRA ANALYSIS

Seismic noise data from the extended short period array located at TFO was analyzed under previous contract F33657-70-C-0100 using a high resolution (HR) spectral technique. This HR technique is of the form  $1/S(\theta)^H \Omega^{-2} S(\theta)$  and is described by Texas Instruments Incorporated (1970). The technique generally gives reasonable wavenumber spectra, but occasionally has spurious secondary peaks. The HR estimates shown here are thought to be satisfactory; they were chosen for comparison because they were readily available. One of the noise samples used in the analysis (designated as "winter" noise) was selected for the evaluation of EG spectral analysis.

#### A. REVIEW OF PREVIOUS ANALYSIS

A significant increase in noise power (approximately 12 dB) was observed for the "winter" sample and was due partially to intense storm activity off the west coast of Alaska. At low frequencies (.12 Hz) a significant amount of surface mode noise generated by the Alaskan storm is evident (Figure IV-1). The surface mode contribution from this storm decreases at higher frequencies and eventually a source to the Northeast becomes the predominant surface mode noise, (at about .70 Hz). At this and higher frequencies, the P-wave noise dominates the spectra. Analysis of the P-wave noise at frequencies around .5 Hz revealed several sources (Figure IV-2).

#### B. EIGENSPECTRA COMPUTATIONS

Based on the previous noise analysis of the "winter" noise sample, the crosspower spectrum matrix computed at the frequency of .284 Hz was selected for the eigenspectra analysis. At this frequency, the multi-directional nature of the P-wave energy is indicated but not resolved. Also a strong surface mode

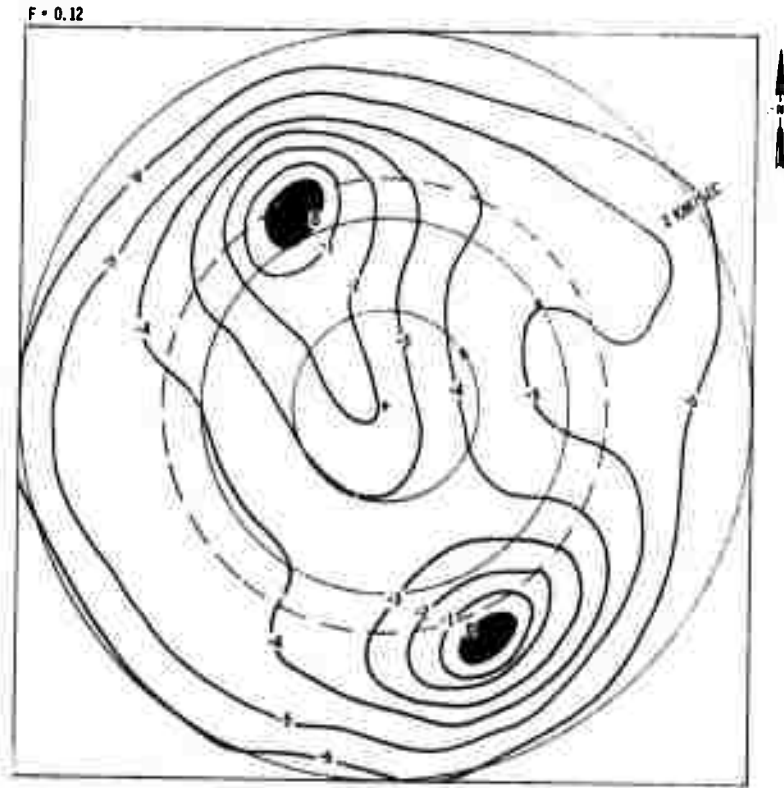


Figure IV-1. TFO Wavenumber Spectrum at Low Frequency (.12 Hz)

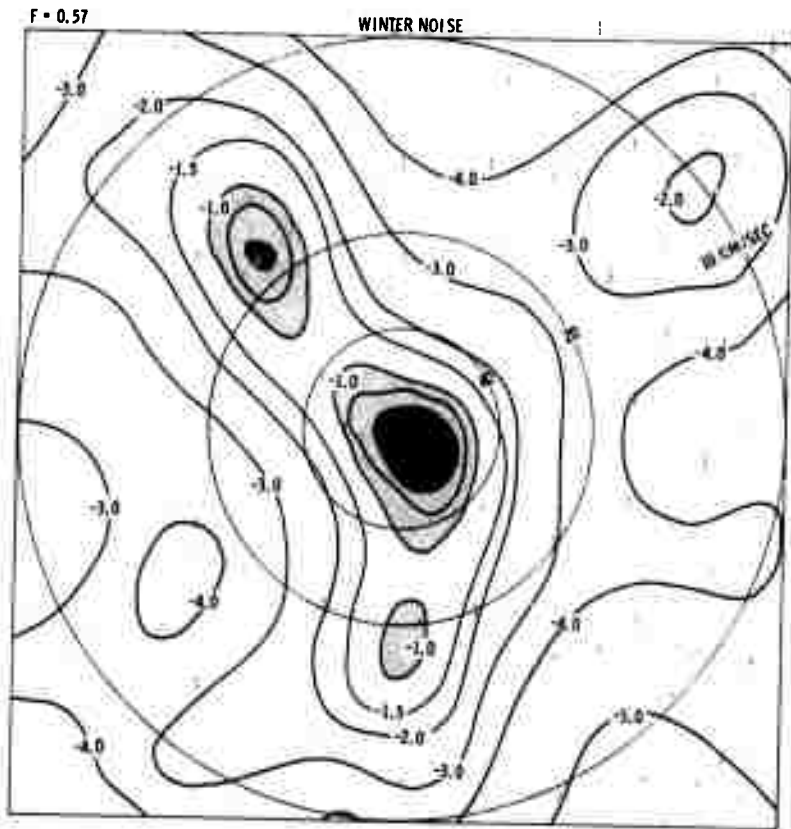
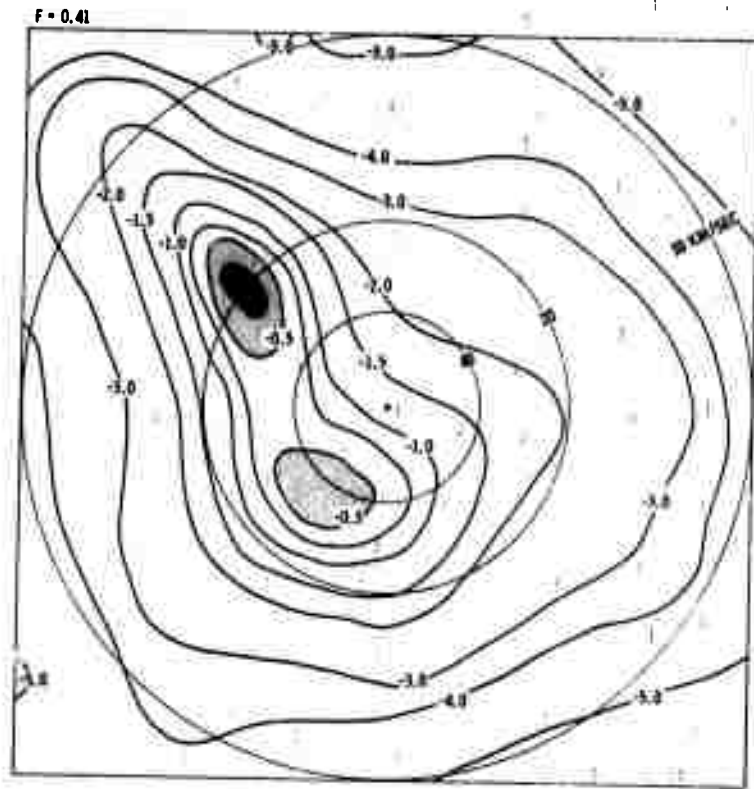


Figure IV-2. TFO Wavenumber Spectra at High Frequency

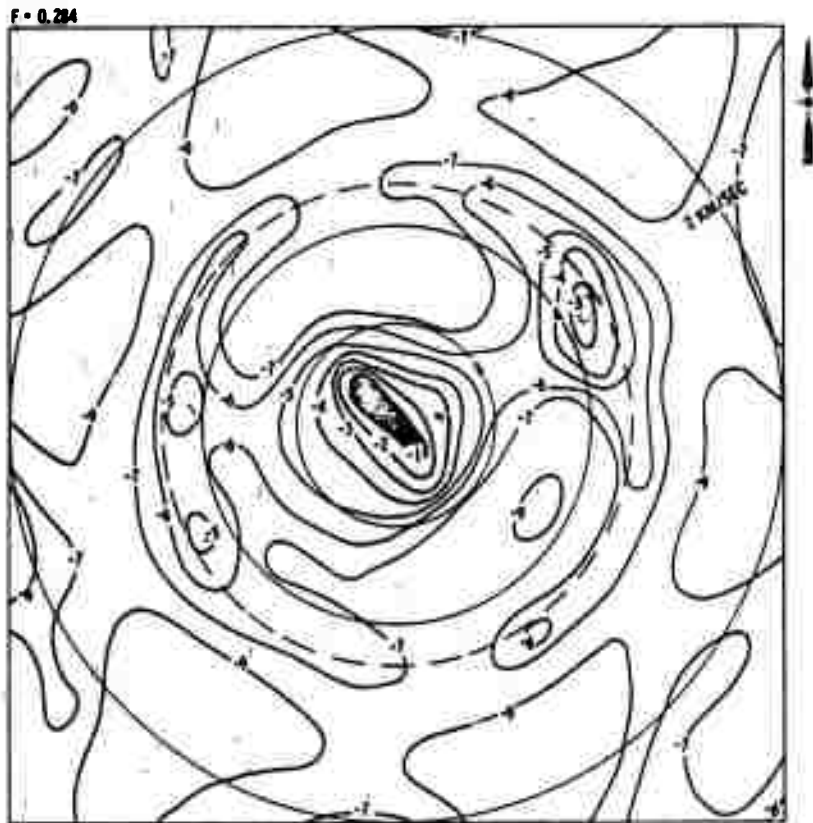


Figure IV-3. TFO Wavenumber Spectrum — Comparison

noise source from the Northeast and a weak one from the West is evident. The HR spectrum computed at this frequency is shown in Figure IV-3; note the isotropic nature of all surface mode noise.

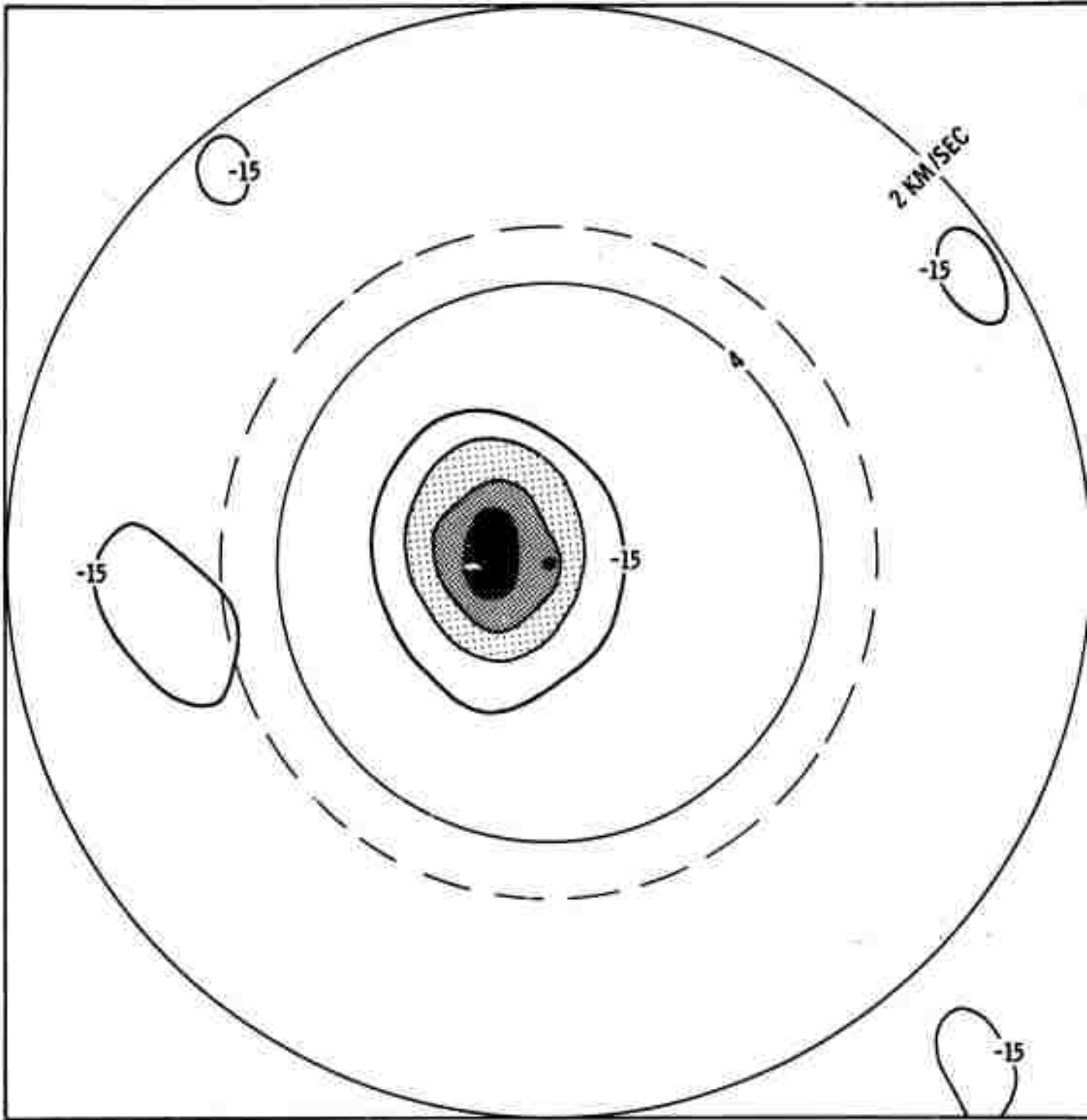
Ten eigenvector-values were extracted from the crosspower matrix. A maximum of 100 iterations were allowed in the algorithm to extract the eigenvalues. If the criterion was not satisfied at that time the vector obtained to that point was accepted and extracted from the matrix. Table IV-1 presents the number of iterations required and resulting eigenvalue for each of the eigenvectors.

TABLE IV-1  
NUMBER OF ITERATIONS AND RESULTING EIGENVALUE

Eigenvector Number	Number of Iterations	Eigenvalue
1	19	11.322
2	23	6.005
3	22	3.654
4	33	2.065
5	64	1.488
6	66	1.240
7	63	1.061
8	100	.902
9	66	.828
10	100	.699

### C. WAVENUMBER ANALYSIS OF EIGENVECTORS

The wavenumber spectrum of each eigenvector was computed and results are compared with the HR spectrum in a previous analysis. The spectrum from the first eigenvector is shown in Figure IV-4. The spectrum shows a very strong peak which corresponds to the dominating P-wave energy from the Alaska storm direction.



— — — SURFACE MODE VELOCITY

-  0-1 db
-  1-3 db
-  3-6 db

Figure IV-4. TFO Eigenspectrum 1

The spectra from the next two eigenvectors (Figure IV-5) show two other distinct P-wave contributions to the noise field which closely agree with the P-wave sources observed at higher frequencies in the previous analysis (See Figure IV-2).

The spectra from eigenvectors No. 4 and No. 5 (Figure IV-6) show peaks corresponding to surface mode energy, propagating from the North-east of the array. The peak powers in the two spectra differ by about 10 degrees, indicating the presence of surface mode sources to the Northeast (or possibly multipath propagation from a single source). Previous HR spectra at the frequency of 0.33 Hz (Figure IV-7) also indicated two surface mode peaks in this direction. This noise may be generated by low pressure activity in the area of Greenland and Eastern coast of the United States.

The next three EG spectra (Figure IV-8) show peaks corresponding to surface mode noise from the west; these also are suggested in the HR spectrum of Figure IV-7. Note that these components are not certain because the EG spectra are showing significant sidelobes.

The spectrum for the last eigenvector extracted (Figure IV-9) has many peaks in the surface mode region, suggesting that the remaining propagating noise is isotropic.

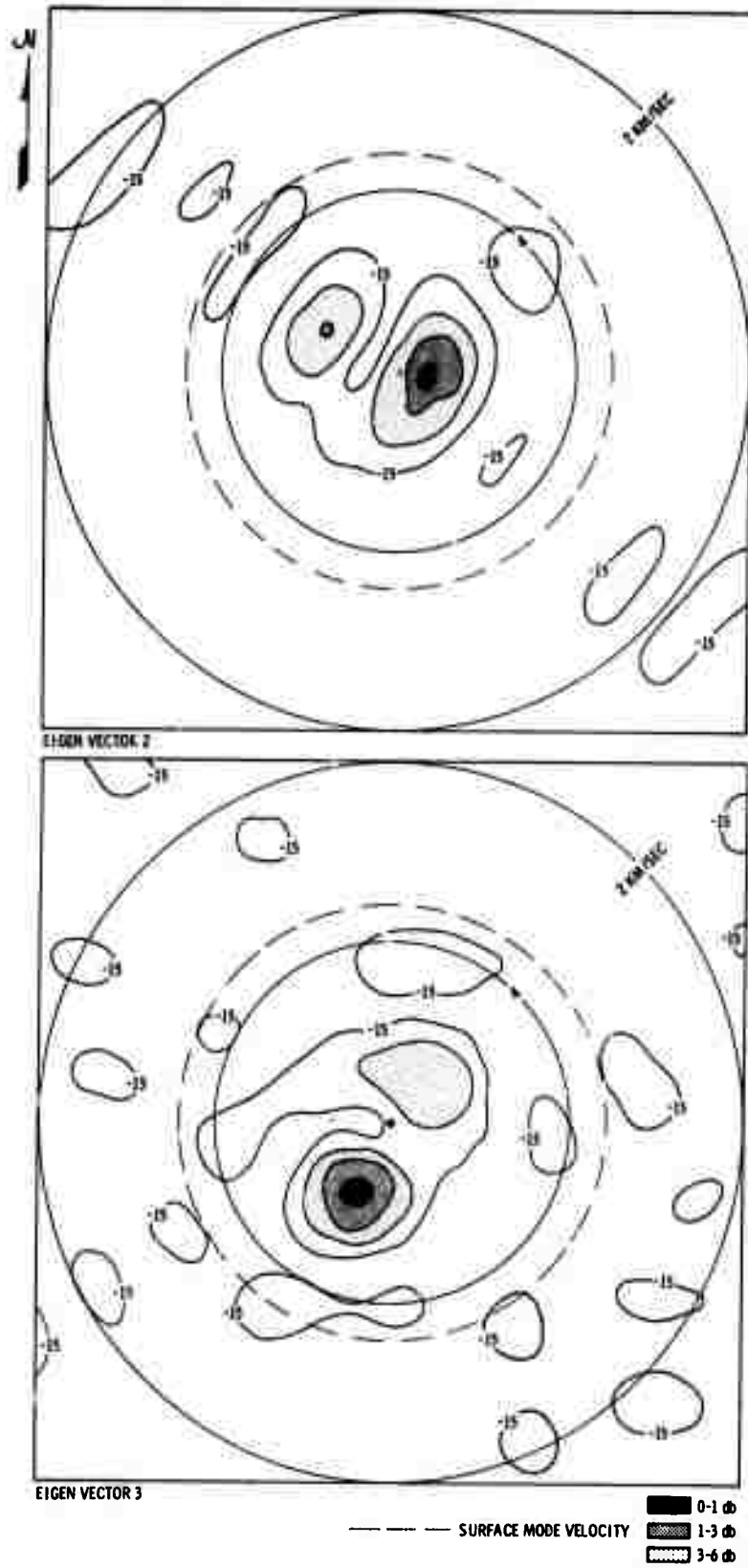


Figure IV-5. TFO Eigenspectra 2, 3

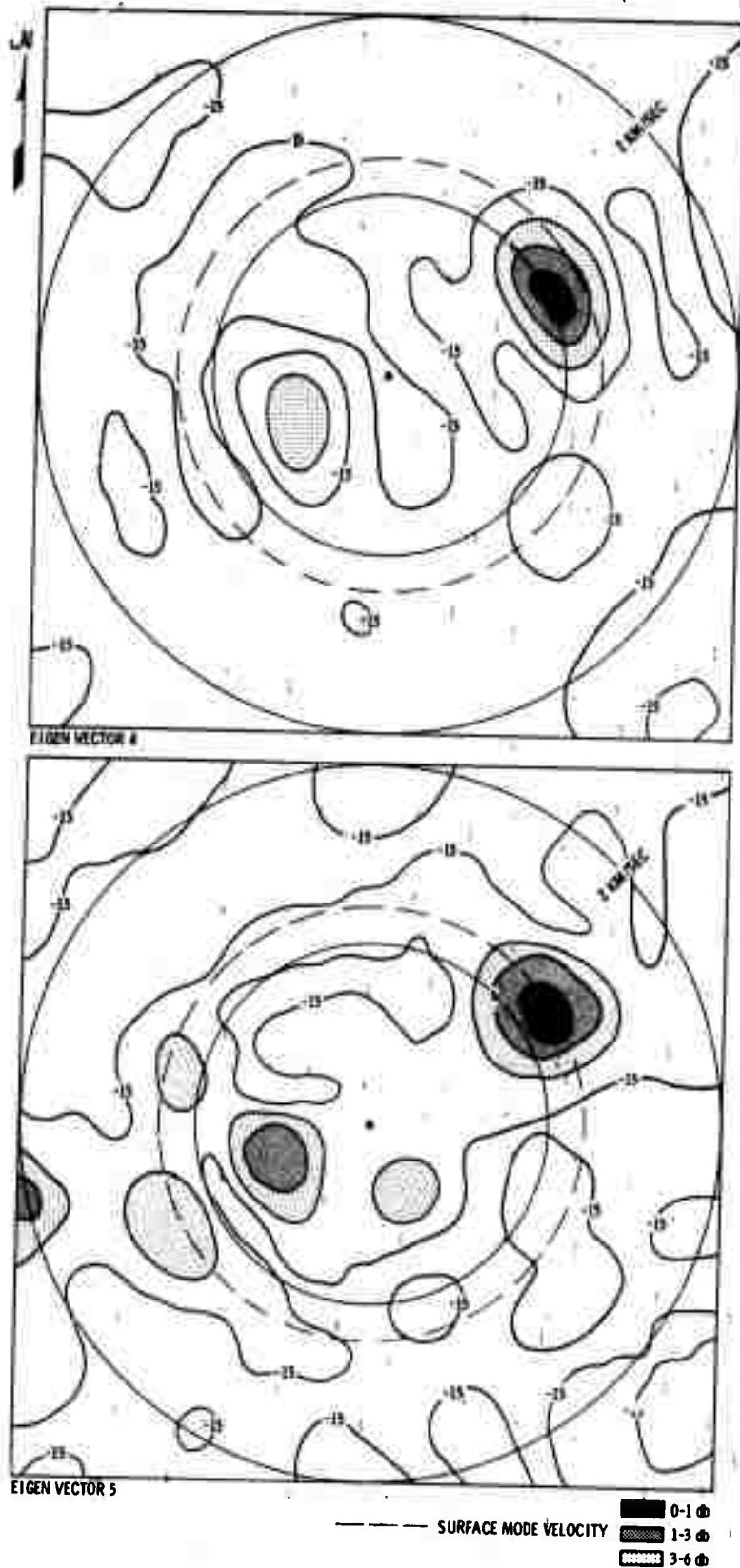


Figure IV-6. TFO Eigenspectra 4, 5

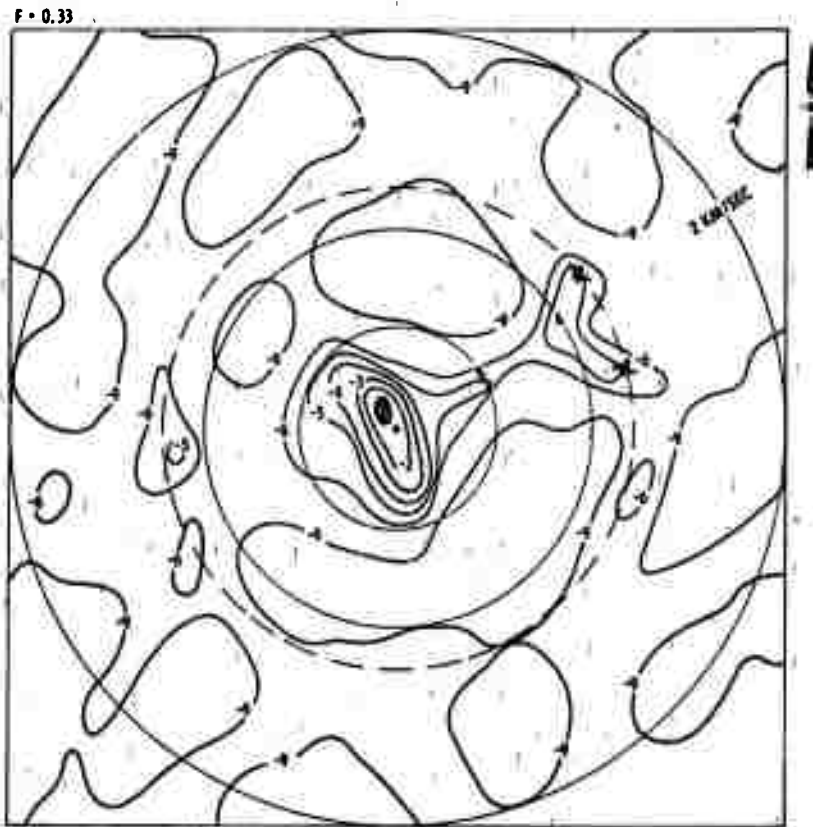


Figure IV-7. TFO Wavenumber Spectrum at 0.33 Hz

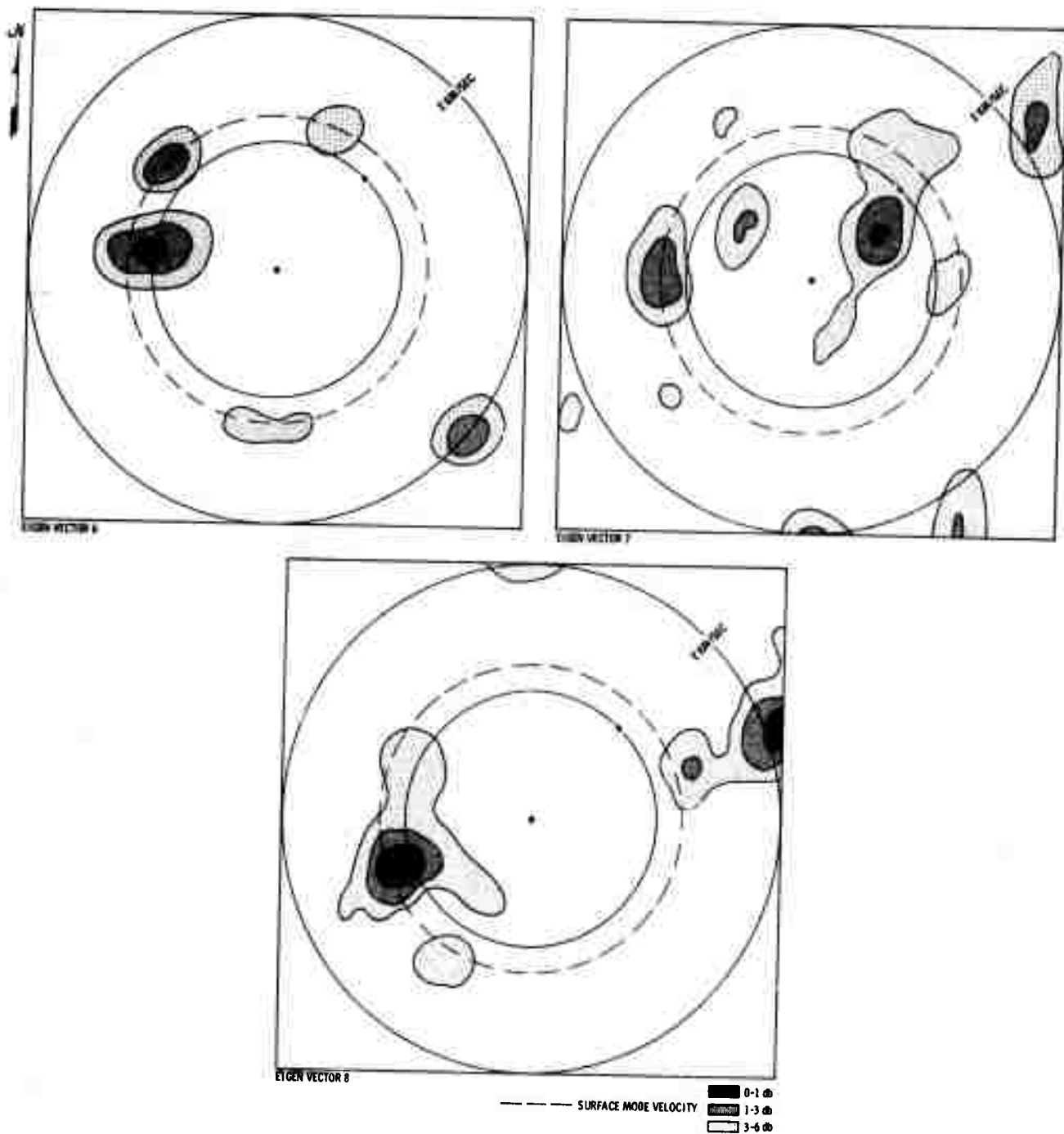


Figure IV-8. TFO Eigenspectra 6, 7, 8

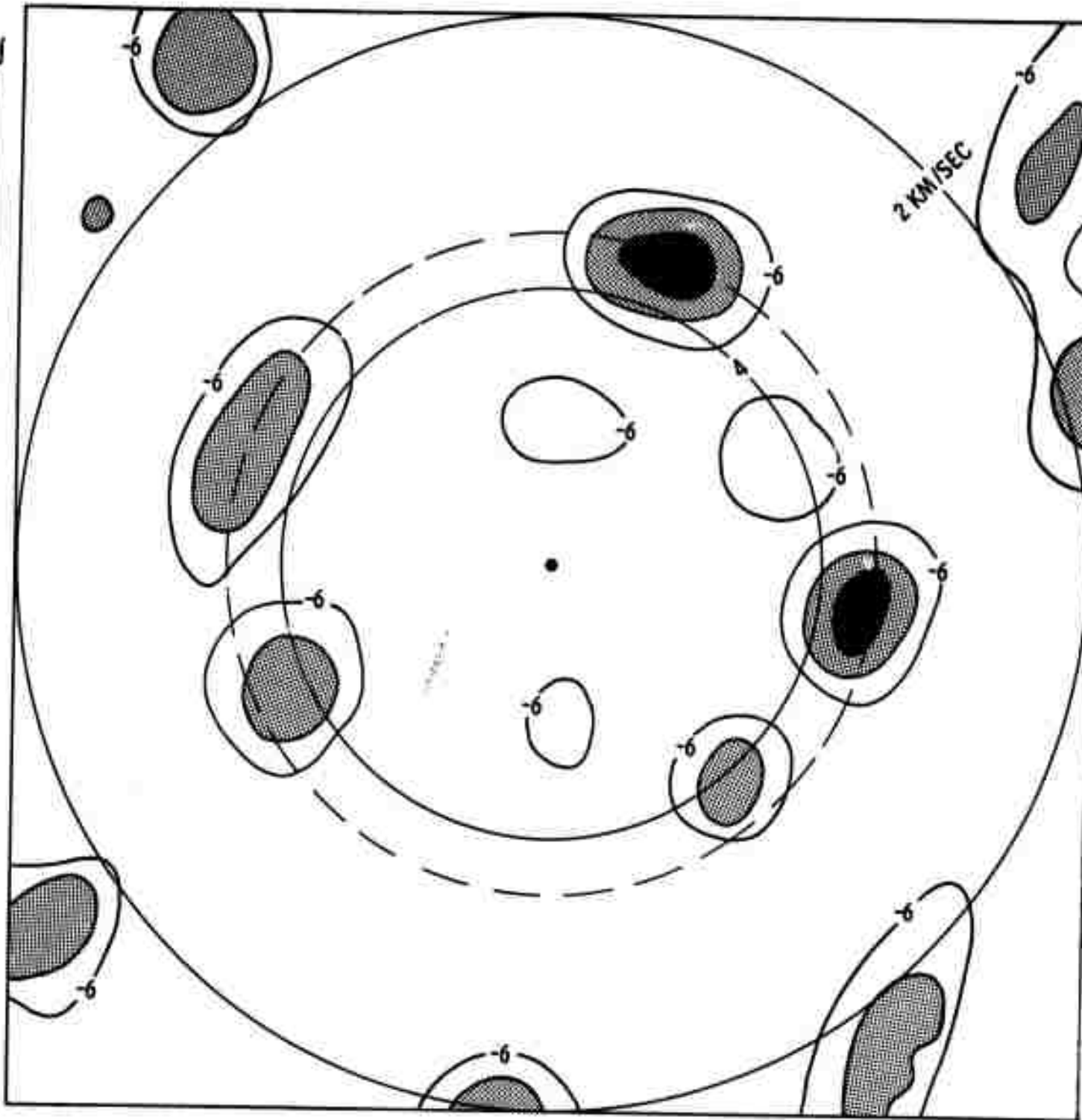


Figure IV-9. TFO Eigenspectrum 9

## SECTION V

### CONCLUSIONS

Four wavenumber spectral estimation techniques, beamsteer (BS), maximum likelihood (ML), maximum entropy (MK) and eigenspectral analysis (EG) have been compared in terms of resolution and stability using synthetic covariance matrices generated for a linear array. In addition, the EG technique, which has not been applied previously in seismology was used on real seismic data and compared with the ML technique applied to the same data. Major conclusions are given below:

1. For the synthetic data the EG technique recovered weak signals best; in certain cases it was capable of recovering signals 50 dB below the largest signal in the covariance matrix. The ML and MK techniques could recover signals 30 dB below the largest signal. The better performance by the EG technique resulted because it is insensitive to random noise.
2. The MK technique showed the best capability to resolve two signals having similar azimuths. For the synthetic example used, the MK technique could resolve two signals  $6^\circ$  apart, but could not resolve two signals  $2^\circ$  apart. The ML and EG techniques could resolve signals  $9^\circ$  but not  $6^\circ$  apart; the BS technique could not resolve signals  $9^\circ$  apart.
3. The stability of all estimates appeared to be good. The BS was the most stable, the EG (at least in the vicinity of the signal directions) seemed to have the next best stability, and the ML and MK techniques appeared to be similar.
4. Application of the EG technique to real seismic data gave interpretable results consistent with HR analysis of the same data. In fact, the EG technique seemed to give better resolution of the propagating noise components.

5. The EG technique appears to be a very valuable tool for array analysis; its insensitivity to random noise is a very important property because real seismic data usually has a significant random noise component which can limit the ML and MK techniques. Possible applications of this technique include separation of overlapping events and array detection.

SECTION VI  
REFERENCES

- Anderson, T. W. , 1958, Introduction to Multivariate Statistical Analysis; John Wiley and Sons Inc. , New York.
- Goodman, N.R., 1967, Eigenvalues and Eigenvectors of Spectral Density Matrices; Seismic Data Laboratory Report No. 179, Contract F33657-67-C-1318, April.
- Owsley, N. L. , 1971, An Aperture Constrained Adaptive Auxiliary Array for Broadband Beam Outputs, Part I - The Central Algorithm; NUSC/NL Technical Memorandum No. 2242, -4-71, January.
- Texas Instruments Incorporated, 1970, Seismic Array Processing Techniques, Final Report, Contract F33657-70-C-0100, 27 August.